AD-A107 341 OHIO STATE UNIV RESEARCH FOUNDATION COLUMBUS F/G 11/6
OPTIMIZATION OF PERFORMANCE OF ARC WELDING USING FLUXES IN WELD--ETC(U)
SEP 81 C E HACKSON, J T HICKEY, M D HAYES N00014-75-C-0666
UNCLASSIFIED NL

END
DATE FILMED
12-81
DTIC

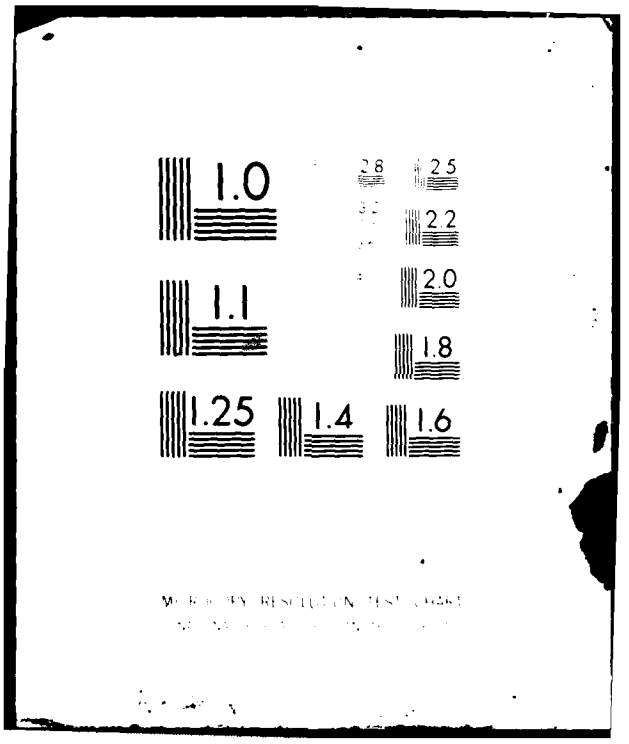
1.0
1.1
1.25
1.4
1.6
2.0
1.8
2.2
2.5

LEVEL II

(12)

NR 031-775

RF Project 760231/784125
(9) Final Report.
1 Feb 75-31 Dec 78,

the ohio state university
research foundation
1314 kinnear road
columbus, ohio
43212

(6) OPTIMIZATION OF PERFORMANCE OF ARC WELDING USING FLUXES IN WELDED SHIP STRUCTURES FROM HY-100 AND HY-130 KPSI.

Clarence E. Jackson, James T. Hickey, and Michael D. Hayes
Department of Welding Engineering

For the Period
February 1, 1975 - December 31, 1978

DEPARTMENT OF THE NAVY
Office of Naval Research
Arlington, Virginia 22217

(15) Contract No. N00014-75-C-0666

(11) September 1981

26736

OPTIMIZATION OF PERFORMANCE OF ARC WELDING USING FLUXES IN WELDED SHIP STRUCTURES FROM HY-100 AND HY-130 KPSI

A Final Report

for the

Office of Naval Research
Department of the Navy
Arlington, Virginia 22217

under Contract No. N00014-75-C-0666

****

High Purity Submerged Arc Welding Fluxes

from

The Ohio State University
Department of Welding Engineering
190 W. 19th Avenue
Columbus, Ohio 43210

August 15, 1981

Abstract

The ability to weld steels with yield strengths over 100 ksi with the submerged arc process has been limited by a lack of fluxes and filler metals specifically designed for this purpose. This research program used commercially available filler wires that have been designed for gas metal arc welding and formulated flux compositions to limit the oxygen pickup in the weld metal. The effect of flux basicity on weld metal oxygen content was investigated. Experimental results with approximately 100 heats of fused flux indicated a definite trend of decreasing weld metal oxygen content with increasing flux basicity. Through the use of basic high purity fluxes, weld metal oxygen content was reduced to a level as low as 80 ppm. The addition of $BaCO_3$ as a mixture or ZrO_2 in the flux formulation was found to reduce the oxygen content of the weld metal.

In these tests the commercial fluxes produced weld metal with adequate toughness but low yield strength. In mechanical testing, the weld metal produced with experimental fluxes showed good tensile properties with inadequate impact values. The coarse microstructure of the last pass in the welds produced with experimental fluxes appears to be made up of untempered martensite, lower bainite, ferrite and proeutectoid ferrite. It is probable that the cracking observed was solidification cracking and may be related to the high phosphorus content of the weld metal. Additions of vanadium and molybdenum in the electrode or as oxides in the high purity flux may be effective in improving toughness.

HIGH PURITY SUBMERGED ARC WELDING FLUXES

Introduction

Studies of the weldability of high strength steels have been extensive. The ability to maintain weld quality and mechanical properties must be assured. The utilization of gas metal arc welding processes has increased the production rate in many applications. Weld quality can be controlled with this process and mechanical properties are generally within specifications. But, this process does not permit a high deposition rate and at times can not be incorporated into the welding schedule due to space or other considerations. For these reasons, the submerged arc welding (SAW) processes and the shielded metal arc welding (SMAW) have been used. The impurities associated with the flux systems in welding have required additional study and improved performance has been obtained with a careful selection of flux ingredients. The development of flux systems with higher basicity assists in the submerged arc welding of steels that are sensitive to impurities such as oxygen and sulfur. Preliminary tests with SAW using available commercial filler metals for the gas metal arc process have shown promising results. Further development of filler metal composition for the submerged arc welding of high strength steels may require a modification of the gas metal arc electrode composition. The approach taken in this research program has been that of using a premium filler wire designed for gas metal arc welding and to modify flux compositions to limit oxygen and silicon pickup in the weld metal. This will lead to a better understanding of the factors controlling slag/metal behavior.

This report deals with two areas which have received attention. The first area is a study of flux composition and its effect on the oxygen content of the weld metal. A review of the effect of higher basicity characteristics of the flux on the weld metal composition and properties is included. The second area deals with the control of the cooling rate of the weld deposit and its effect on the mechanical properties of the weld metal. These studies may lead to better understanding and new concepts which will assist in the fabrication of structures using high strength steels.

SUBMERGED ARC WELDING CHARACTERISTICS

The submerged arc process produces a weld by heating with an electric arc or arcs between the bare metal electrode or electrodes and the work. The welding is shielded by a blanket of granular fusible material placed on the work. Pressure is not used and filler is obtained from the electrode and sometimes from a supplementary metal powder addition or from the flux itself. Submerged arc welding is characterized by use of high welding currents; the current carried in relation to the cross-sectional area of the electrode is several times as great as in manual covered electrode welding. Because of this the melting rate of the electrode and the speed of welding are increased.

The submerged arc is an arc enclosed in a conductive shell as shown in Figure 1. The major current is carried from the electrode to the weld crater through the vapor in the arc zone; in normal operation part of the current is also carried across the space through the molten flux enclosing the arc cavity. At room temperatures, the granules of

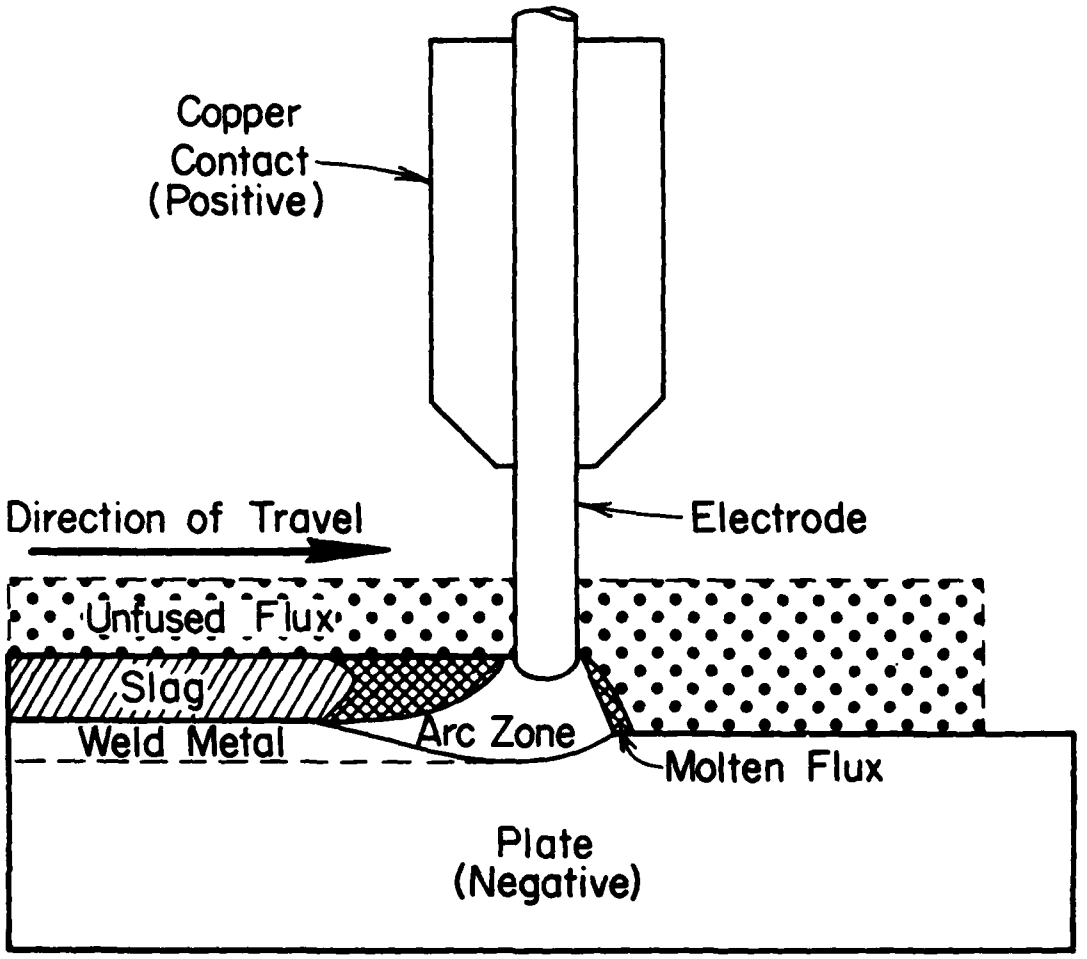

Figure 1. Schematic of Submerged Arc Welding Process.

submerged arc fluxes are non-conductors, but with an increase in temperature the electrical resistance of the flux decreases and becomes highly conductive. At the temperatures in the welding zone (1), a welding slag must have sufficient viscosity to give it impermeability to atmospheric gases and to prevent it from running away from the molten metal. At the same time, the viscosity must be low enough to permit gases to be released from the molten metal. The effect of temperature on viscosity and electrical resistance for a typical calcium-silicate submerged arc flux is given in Figure 2. The electrical resistance at temperatures above the melting temperature of steel is low enough so that fairly high currents may be carried by the molten flux arc enclosure. The distribution of the current in the parallel branches of the arc zone depends upon the composition of the flux and the arc vapor. If the molten flux takes the bulk of the current, an electro slag operation results and no arc cavity will exist. An oscilographic record of the arc action (2) can be obtained if an alternating current power supply is used. In this case, the record shows a sine wave form for an electro slag or for a flux carrying the current in a linear resistance pattern. (Fig. 3a). On the other hand, an arc with a conducting shield of molten flux will show a modified sine wave (Fig. 3b) and finally, in an open arc or a molten flux enclosure which carries little or no current, a characteristic arc voltage trace (Fig. 3c) will result. It is obvious that the voltage characteristic is one of the significant factors in the electrical operation in the welding zone. The almost instantaneous rise in voltage in a peak at the beginning of each half cycle indicates the ignition potential which is a characteristic

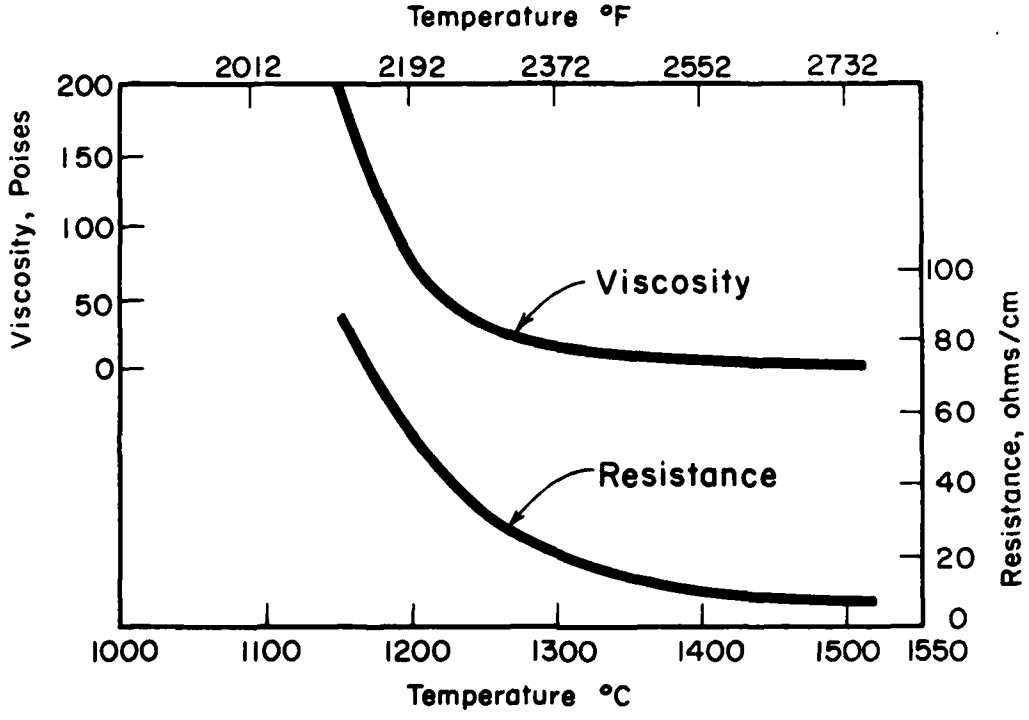

Figure 2. Effect of Temperature on Viscosity and Electrical Resistance for a Typical Calcium-Silicate Submerged Arc Flux (1).

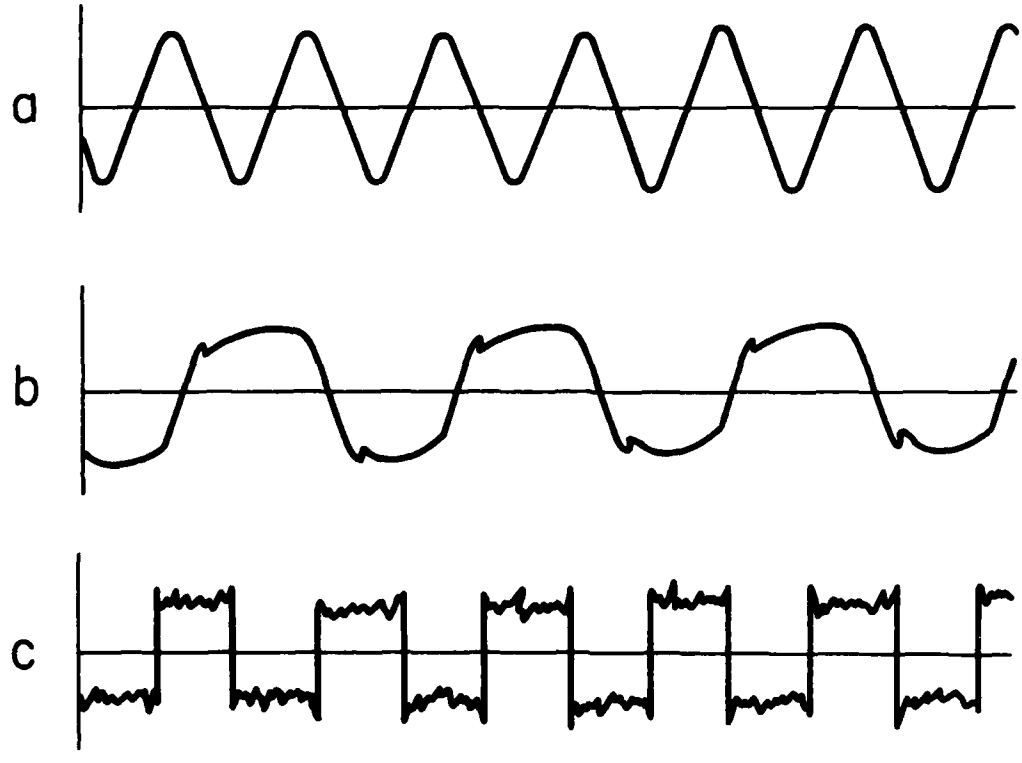

Figure 3. Oscillograms showing voltage trace for a. conduction in resistance pattern, b. conduction through a molten flux in parallel to the arc and c. a typical welding arc (2).

of alternating current arcs. For a direct current power supply this reignition phenomena exists only at the start of the arc action. Conduction in an arc takes place through a gaseous column which has a high electrical conductivity. The arc contains in series the plasma, cathode and anode regions. The conductivity of the plasma between the electrodes is maintained by thermal ionization at a high temperature. All experts agree that the conditions in the region of electrical contact between the plasma and the electrodes are quite different from those in the plasma. In both the anode and the cathode region since the temperature must drop from the high value of the plasma to the relatively low value at the electrode surfaces, high thermal gradients exist. A concentration of charged carriers in the anode and cathode regions give rise to a nonlinear potential or voltage distribution along the arc axis. The melting rate of the electrode and work piece is related to the current which is used in the welding operation. With the electrode connected to the positive terminal the measurements of the amount of electrode melted in the arc will depend on the anode energy plus the I^2R heating of the electrode extension. This energy combined with the cathode energy results in the melting of the weld metal for the joint. For a given current the quantity of flux which is fused increases linearly with voltage as shown in Figure 4. It can be shown that for many commercial fluxes approximately 0.4 to 0.5 kwh will be required to melt 1 pound of flux in the weld zone. For example in Figure 4, an increase in voltage from 20 to 40 volts with a welding current of 500 amperes results in an increase in flux consumption of approximately 0.4 lb/min. The power used is 20 x 500 or 10,000 watts

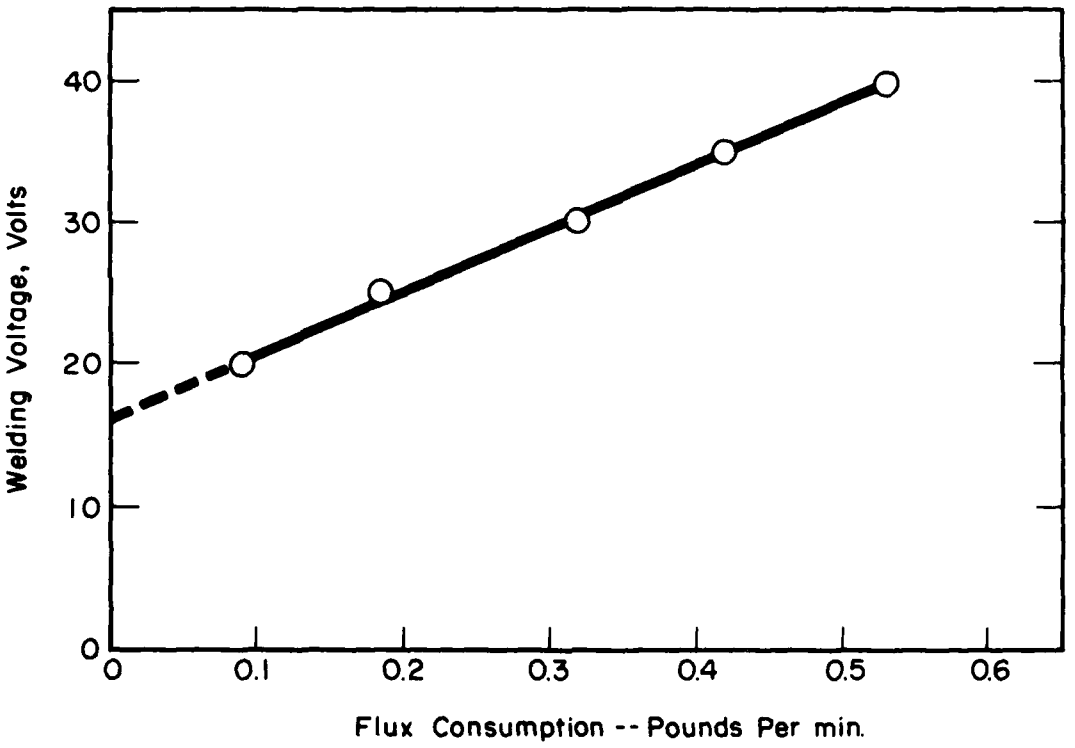

Figure 4. Effect of Welding Voltage on Flux Fused per Minute for a Calcium Silicate Submerged Arc Flux with a Current of 500 amperes.

which calculates to 0.42 kwh per pound for melting the flux in the welding operation. This is similar to the energy required for the commercial production of a fused flux for submerged arc welding in an electric melting unit. The slag/metal reactions in the arc cavity will depend on the temperature and composition of the flux. Thermal conditions exist which can be measured and have been studied by many investigators (3), (4). One of the earliest studies is that by Claussen (5) who describes slag/metal reactions in the weld zone; he suggests that the temperature in the weld zone may be predicted from reaction constants used in steel-making. Claussen suggests an effective temperature in the order of 1600°C (2910°F). Christensen and Chipman (6) in their work on slag/metal reactions in arc welding with E6020 type electrode coating conclude that the effective temperature is slightly below 2000°C (3630°F). Effective maximum and average temperature and the distribution of silicon and manganese between slag and weld metal is pointed out by Christensen. It is also stated that the mixing of the slag and metal in weld puddle must be very efficient to permit equilibrium to be approached in the time available. Erokhin (7) suggests temperatures of 2000 to 2400°C which are higher than those reported by other investigators. Calorimetric measurements have been reported by Jackson (1) which indicate the temperature of 1750°C in the submerged arc welding puddle. Frumin (8) measured the maximum temperature of 1695°C during the submerged arc welding of mild steel. Japanese investigators (9) have pointed to the fact that the effective temperature in the weld zone may be in the order of 1770 ± 25°C. In spite of the extensive work that has been carried out, the complex fluxes undoubtedly will show a variation

in the reaction temperature that exists. The actual effective temperature must be dependent upon the time and slag/metal ratio. In the submerged arc process it has been shown that the quantity of flux usage increases with voltage in the weld zone. The melting rate of the electrode is dependent on the current level and is independent of voltage. Hence the slag/metal weight ratio increases with voltage and this in turn influences the weld metal analysis. Undoubtedly, the oxygen content of the molten weld metal and the solidified weld metal will be dependent upon the reaction temperature that is present. The effective time-temperature relationship which requires close control of welding procedures will be important in maintaining the mechanical properties of the weld metal in the submerged arc welding of high strength low alloy steels.

Objectives

The primary objective of this research program is a study of high purity submerged arc fluxes. The complexity of flux systems in slag-metal reactions requires the use of engineering references or standardization from which conclusions may be drawn. In this investigation flux basicity is used as one criterion in order to study welding performance. Specifically, the effect of flux basicity on weld metal oxygen content is investigated. The objectives are as follows:

1. Review the relationship between flux constituents, basicity and oxygen content of the submerged arc weld metal.
2. Investigation of the MgO-Al_2O_3-SiO_2 system in order to determine compositional ranges suitable for submerged arc fluxes.
3. Study the relationship between fused flux raw material purity and weld metal quality.
4. Prepare mechanical test plates in order to establish areas of adequate performance and further concern for development.

The end result of this study should be a better understanding of the effects of raw material purity and composition on fused flux performance and the oxygen content of the weld metal.

Effect of Flux Basicity on Oxygen Content

One of the engineering concepts which has been widely applied to flux technology in steel making is that of basicity. The use of base/acid terminology has served to distinguish the overall nature of the various slags used in steelmaking. The oxides such as CaO, MgO, MnO and FeO, which break down the anion complexes in the flux are known as the network modifiers and are said to be basic oxides. The oxides of SiO_2, Al_2O_3, etc., which form anion complexes in fluxes, such as silicate and aluminate anions, are said to be acid oxides. The ratio of molar concentrations of basic oxides to those of the acidic oxides is called the basicity of the slag.

In the simplest sense basic oxides react with acids to form salts, while acidic oxides react with bases to form salts. Amphoteric oxides can do either depending on the relative basicity or acidity of the flux composition. The division of flux and slag components within the groups of basic, amphoteric and acidic oxides may be as follows (10):

Basic Oxides	Amphoteric Oxide	Acidic Oxides
FeO	Al_2O_3	SiO_2
MnO	Cr_2O_3	Cr_2O_3
CaO	MnO	TiO_2
MgO	TiO_2	Al_2O_3
Na_2O		ZrO_2
K_2O		

In a discussion of oxide stability effects, Jackson (1) suggests that many times the oxidizing ability of a welding flux is mistakenly thought to be related to the basicity or acidity of the slag. The most popular contention is that acid slags oxidize elements such as chromium while basic slags do not. The basicity or acidity of a slag is related to the ease with which the component oxides dissociate into a metallic cation and an oxygen anion. Oxides which dissociate easily are termed basic, while those which dissociate only to a small degree are termed acid.

From the above discussion it is suggested that there is no absolute scale of basicity. However, the broad distinction between basic alkali-earth metal oxide slags and acid silicate slags remains, since in high temperature nonmetallic fluxes ions such as Ca^{2+}, Mg^{2+} behave in a basic manner by virtue of their donation of electrons to acid ions such as SiO_2^{4-} and $Al_2O_3^{3-}$. In between these easily distinguishable extremes the definition of acids and bases becomes less clear, which partially explains the difficulty in explaining the effects of amphoteric oxides and transition metals.

Even though there are theoretical limitations to characterizing flux systems by base/acid ratios, empirical relationships have been established which when used in the proper perspective can provide valuable performance guidelines for submerged arc fluxes.

It is to be noted that in the formulation of submerged arc fluxes exact stoichiometric ratios seldom give satisfactory welding performance. This is true even in the binary calcium-silicate or manganese-silicate compositions. Eutectic compositions which provide the lowest melting

temperature in the phase diagram generally require modification in order to give the desired welding operations.

The chemical potential, or oxidizing ability of a flux is related to the ease with which its component oxides can be reduced. A flux composed of easily reduced oxides will provide an alloy addition to the weld metal. The stability of a component oxide in a welding flux will influence the oxygen content of the weld metal which in turn will be a factor which influences the mechanical properties of the weld metal.

The oxides which are easily reduced, notably the oxides of iron, manganese, and silicon, may also be reduced by metallic alloying elements such as aluminum or titanium. The products of the reaction are metallic iron, manganese or silicon which are added to the weld metal and oxides of the alloying elements, which dissolve into the slag. As shown in Figure 5, a modest addition of an easily reduced oxide of manganese to a flux insures adequate pick-up of manganese in the weld metal while the more stable SiO_2 is chiefly maintained in the flux up to almost 40 percent.

The reactions between molten metal and slags have been under extensive study in the steel-making industry since the time and temperatures involved can be measured accurately and reactions may go to equilibrium. However in welding applications using fluxes, the short times and high temperatures encountered together with the more complex flux formulations complicate the slag/metal reactions. Davis and Coe (10) suggest that silicon, phosphorus, manganese and carbon are removed from the weld metals by oxidation and transferred to the slag or expelled as gas. On the other hand the molten weld pool may be deoxidized by the addition of ferroalloys

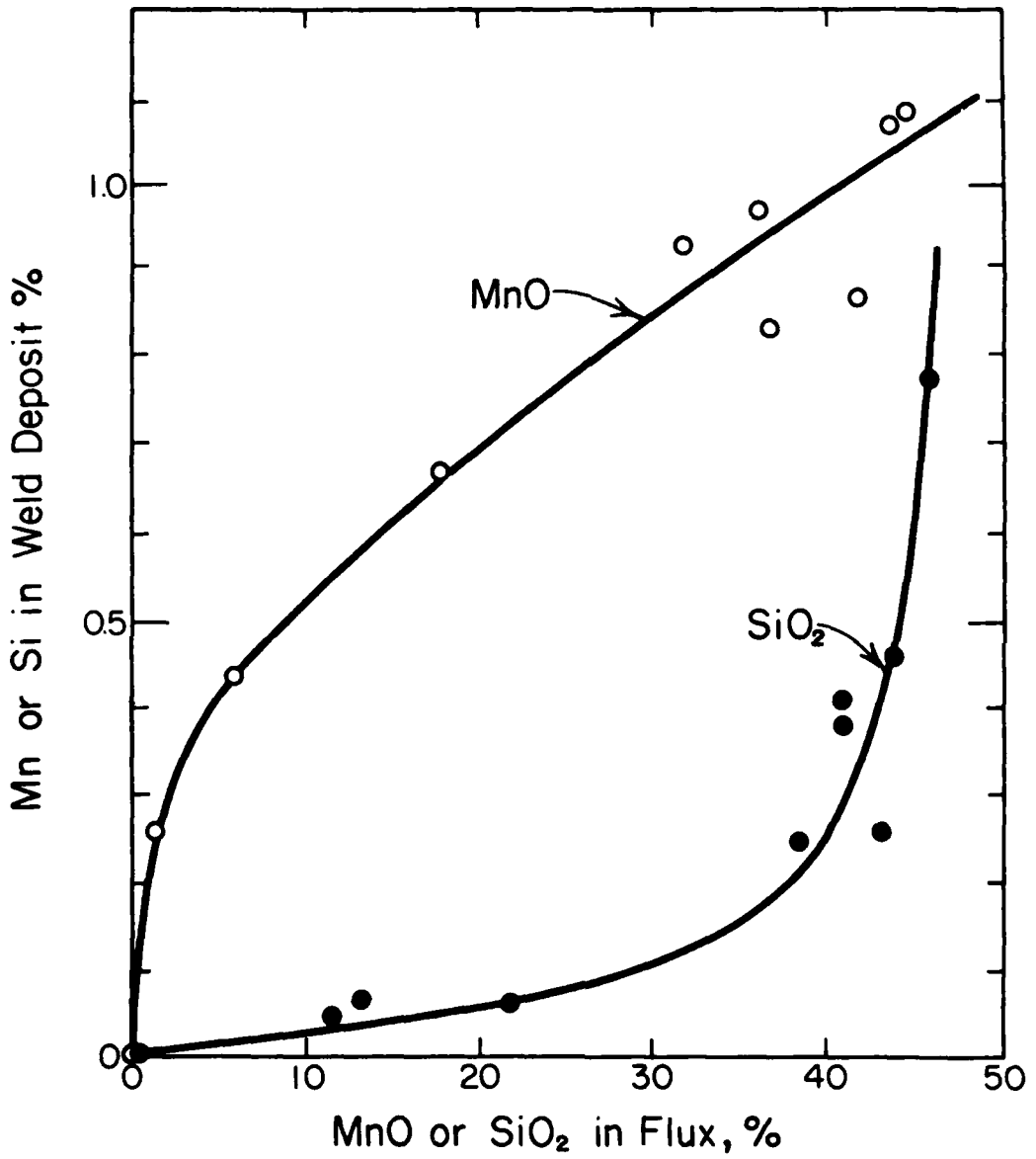

Figure 5. Relation of MnO and SiO_2 in Flux to Mn and Si in Weld Deposit (1).

containing manganese or silicon. In welding flux design use is made of tables of oxide formation energies and energies of reaction (Fig. 6 and Table 1) (11).

Oxide functions may be related (12) to flux design in the following manner: the chemical potential, or oxidizing ability, of a slag is related to the ease with which its component oxides can be reduced. It is described by stating the partial pressure of oxygen which is necessary to prevent decomposition of the component oxide into a metallic element and molecular oxygen; stable oxides require a relatively low partial pressure of oxygen while the less stable oxides permit higher partial pressures of oxygen. The heat of formation ($-\Delta H$) in kilo calories per gram mole for a number of compounds used in flux formulation is given in Table 1. In complex flux compositions which are specified in weight per cent, the effect of a gram weight is obtained by dividing the gram mole by the molecular weight. This is shown in Table 1. It is obvious that a flux composed of easily reduced oxides will be more aggressive towards an alloying element than one with a more stable oxide because the concentration of molecular oxygen in the slag is higher. For example in Fig. 7, adding 5% Cr_2O_3 and 0.75% MoO_3 to a calcium-silicate submerged arc flux modified with Al_2O_3 and MgO tended to stabilize the SiO_2 in the flux thus decreasing the silicon content of the weld metal.

Composition of Submerged Arc Fluxes

Through the long development of covered electrode technology the lime type basic coating has taken over first place in U.S. production. Weld metals with lower oxygen content and improved impact properties have been obtained. The success of the basic coating has raised the question of

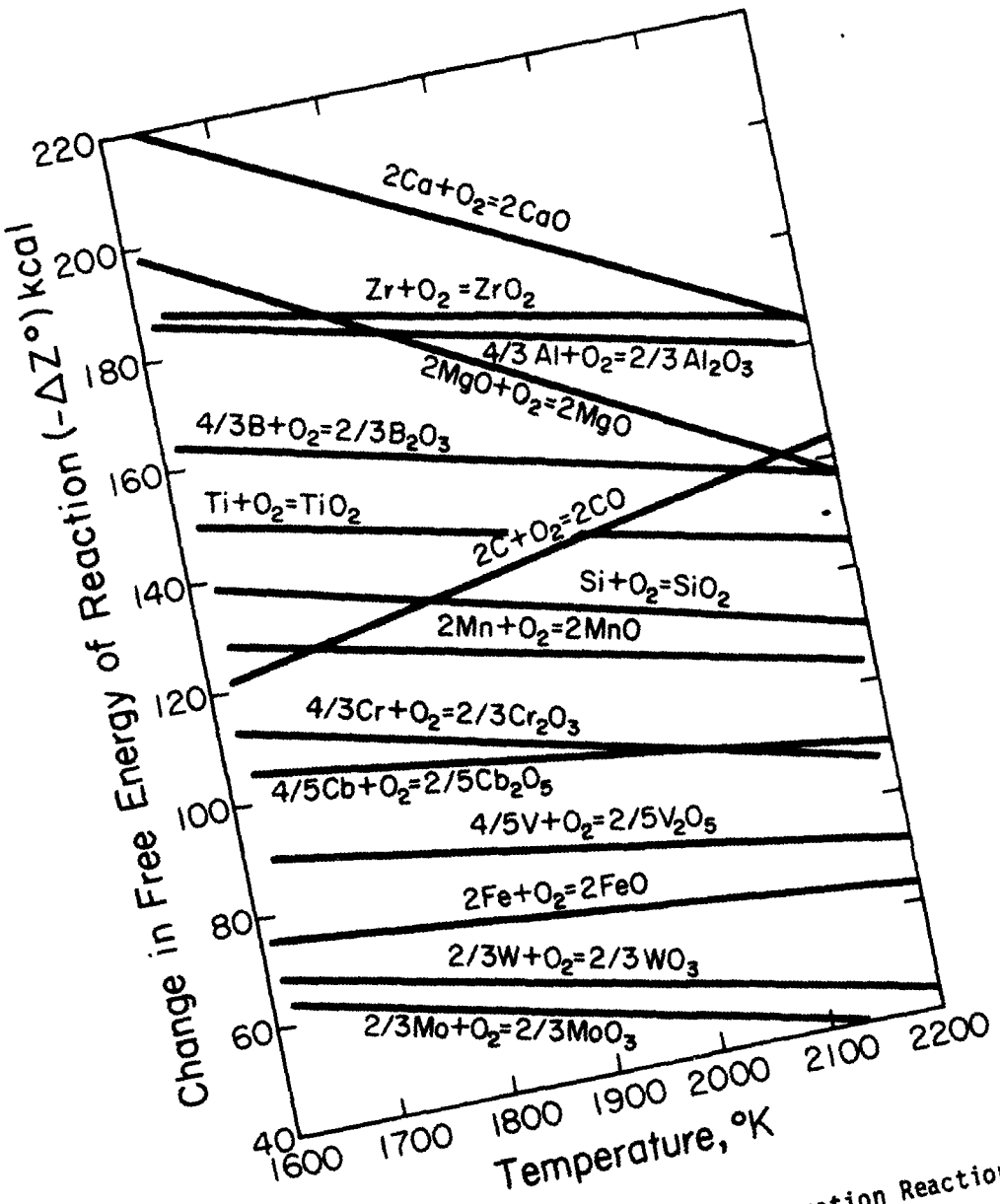

Figure 6. Change in Free Energy of Oxide Formation Reactions (12).

Table 1

	-ΔH*	Molecular Weight	-ΔH/gram
MoO_3	38700	143.94	- 268
NiO	55940	74.71	- 748
FeO	62050	71.85	- 863
BaO	139000	153.34	- 906
CO	26770	28.01	- 955
MoO_2	139200	127.94	-1088
MnO	95400	70.94	-1344
Cr_2O_3	267750	151.99	-1761
Na_2O	117700	61.98	-1899
ZrO_2	255020	123.22	-2069
CaO	153500	56.08	-2737
TiO_2	224330	79.90	-2807
SiO_2	227700	60.08	-3790
Al_2O_3	402300	101.96	-3945
CaF_2	315500	78.08	-4040
MgO	176800	40.31	-4386

* Units: kilo-calories per gram mole (11).

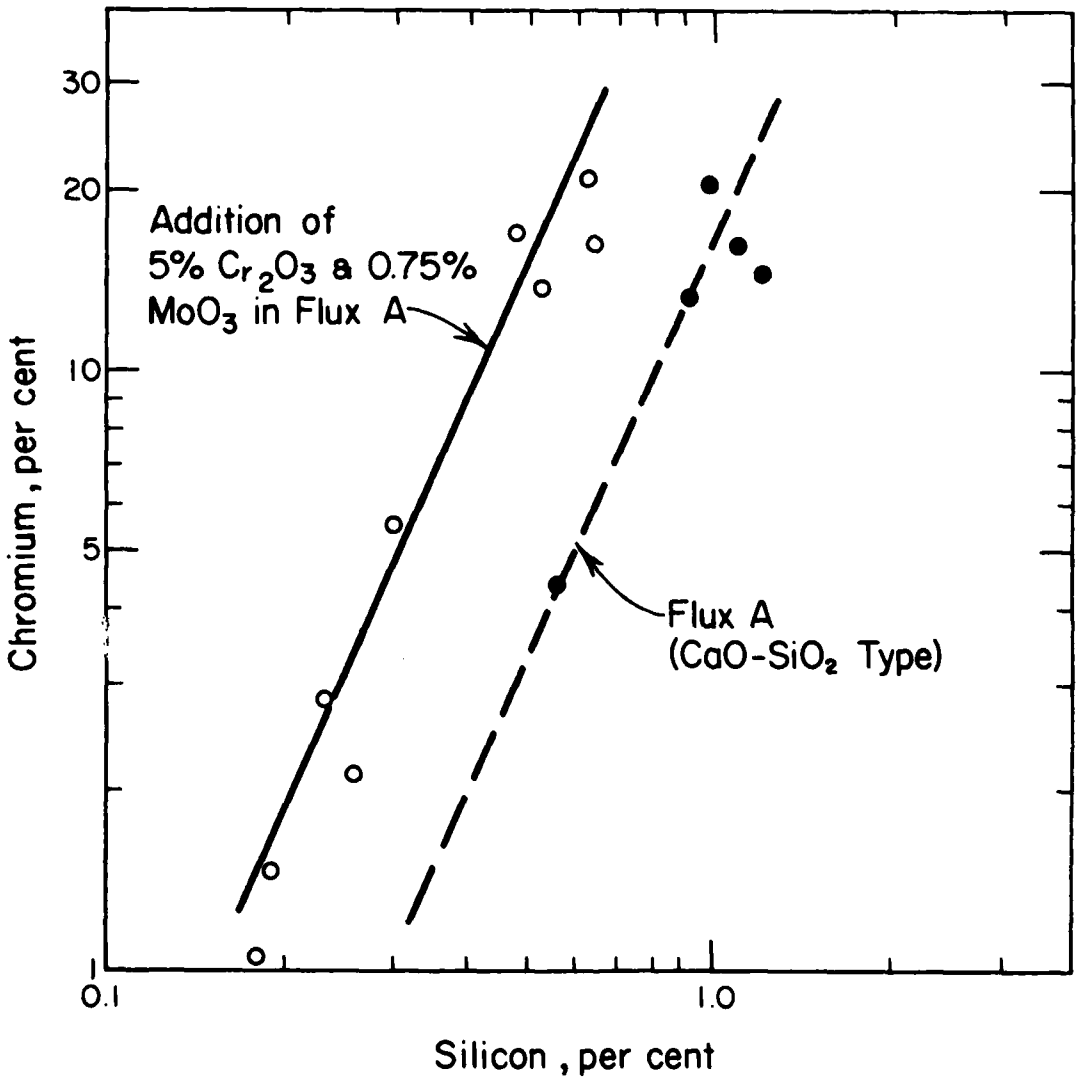

Figure 7. Reduction of Silicon content of Weld Metal by the Addition of Cr_2O_3 and MoO_3 to a Calcium-Silicate Flux (13).

basicity in other welding flux systems. In studies of submerged arc fluxes attempts have been made to quantify the basicity of a flux based on the chemical composition. In many studies (14), (15), (16) often the analyses of the flux based on the material formulation is used. Formulas made up using commercial minerals vary in purity with undetermined tramp elements being neglected. Difficulties are often encountered by the chemist in analyzing these materials due to the cost and skills required for studies of silicate samples. Standard samples for comparison of techniques are seldom used and comparison of the results presented by various investigators is difficult. Since accurate chemical composition analyses are not often available, the industry has not formed an accepted standard for specifying basicity. However basicity, as calculated using charge analyses, can serve as a guide in much the same manner as other indices such as "carbon equivalent" or "hardenability".

The following molar formula has been used by one of the authors for flux production and formulation for several decades.

$$\text{Basicity} = \frac{\text{NMgO} + \text{NCaO} + \text{NMnO} + \text{NFeO} + \tfrac{1}{2}\text{NAl}_2\text{O}_3}{\text{NSiO}_2 + \text{NTiO}_2 + \text{NZrO}_2 + \tfrac{1}{2}\text{NAl}_2\text{O}_3}$$

This differs from the widely quoted and referenced IIW system (17), (18) in that it does not include the diluent CaF_2 in the calculation. The inclusion of CaF_2 is not important when this material is in the 5 to 10% range. However, the reaction in the weld zone has been overemphasized since even in the range of 20 to 30% CaF_2 required in present day basic fluxes, CaF_2 is stable and the retention of fluorine in the welding slag is almost complete.

In the production and use of fluxes containing CaF_2 difficulty has sometimes been encountered due to the formation of fumes. Since CaF_2

has a boiling point of approximately 2500°C these fumes are the product of reaction of CaF_2 with other components in the flux. The most common irritating product has been identified as SiF_4 which is assisted in its formation by the presence of moisture.

$$2CaF_2 + 2H_2O \rightarrow 2CaO + 4HF$$

$$\underline{4HF + SiO_2 \rightarrow SiF_4 + 2H_2O}$$

$$2CaF_2 + SiO_2 \rightarrow 2CaO + SiF_4\uparrow$$

Tuliani et al (18) show an increase in the CaF_2 in the fused slag in some cases where there has been a reduction of several percent in the SiO_2 resulting in an increase of Si in the weld metal. A reproduction of tabular data from Tuliani et al is shown in Tables 2 and 3. Increasing flux basicity lowered the weld metal sulphur content, decreased the oxygen and silicon contents of the weld metal which increased the toughness and lowered the nonmetallic inclusion content. CaF_2 was found to decrease Si content in the weld metal and high alumina fluxes (40% Al_2O_3) yielded a weld metal with Al contents of 0.037%.

Garland and Kirkwood (19) have also shown the beneficial effects of basic fluxes on weld metal toughness. Molybdenum additions of up to 0.5% in the filler wire were reported to yield dramatic improvements in toughness for low heat input welds made with basic fluxes.

Bennet (20) found that welds made with basic fluxes usually had poorer slag removal and bead appearance but better mechanical properties. It was also found that basic fluxes containing oxides of Ca and Mg in excess of their stoichiometric composition were hygroscopic and should be dried in a manner similar to basic covered electrodes.

Mills and Keene (21) point out that slags for electroslag refining serve three primary functions:

Table 2

Chemical Analyses of Submerged Arc Weld Metals (wt. %) (18).

Weld Code	C	Mn	Si	S	P	Ni	Cr	Mo	V	Ti	Al	Oxygen	Nitrogen
A1	0·12	0·58	~1·3	0·015	0·017	<0·10	<0·10	<0·10	<0·10	<0·05	0·005	0·088 (1) 0·080 (2)	0·008 (1) 0·010 (2)
B1	0·07	~1·7	0·32	0·012	0·018	<0·10	<0·10	<0·10	<0·10	—	0·005	0·022 (1) 0·027 (2)	0·008 (1) 0·010 (2)
C2	0·06	1·10	0·83	0·037	0·029	<0·10	<0·10	<0·10	<0·10	—	0·037	0·077 (2)	0·009 (2)
D2	0·05	1·19	1·04	0·031	0·018	<0·10	<0·10	<0·10	<0·10	—	0·005	0·086 (2)	0·009 (2)
E3	0·13	1·07	0·24	0·014	0·021	<0·10	<0·10	<0·10	<0·10	—	0·02	0·018 (1) 0·038 (2)	0·011 (1) 0·014 (2)
F4	0·07	0·54	0·16	0·014	0·028	<0·10	<0·10	<0·10	<0·10	—	0·019	0·025 (1) 0·034 (2)	0·004 (1) 0·004 (2)
F5	0·06	0·98	0·52	0·011	0·018	0·84	<0·10	<0·10	<0·10	—	0·005	0·027 (2)	0·010 (2)
G6	0·10	0·86	0·76	0·014	0·019	1·44	0·19	<0·10	<0·10	<0·05	<0·005	0·051 (2)	0·008 (2)
H6	0·13	0·87	0·75	0·016	0·019	1·25	0·20	<0·10	<0·10	<0·05	0·018	0·029 (2)	0·006 (2)

Analysis carried out by:
(1) Rideadale & Co. Ltd., Newham Hall, Middlesbrough
(2) BISRA, Sheffield.

Table 3

Analyses of Commercial Submerged-Arc Welding Fluxes and Slags (wt. %) (18)

Type of Flux	Sample Code	SiO_2	Al_2O_3	TiO_2	CaO	MgO	MnO	FeO	Na_2O	K_2O	Li_2O	BaO	SrO	CO_2	CaF_2	Ni	NiO	Total	★ Basicity
Fused	Flux A	58·60	0·76	0·29	28·98	8·35	0·30	0·24	0·07	0·16	ND	0·026	0·008	Nil	3·06	ND	—	100·89	0·99
	Slag A1	53·90	<1·50	0·28	24·63	8·30	4·30	3·06	0·24	0·19	0·19	ND	<0·04	Nil	2·88	—	0·22	97·93	0·96
Fused	Flux B	35·10	0·71	0·06	35·99	0·30	9·00	0·26	4·22	0·31	ND	0·384	0·013	Nil	12·12	ND	—	98·46	1·63
	Slag B1	37·40	<1·50	0·28	32·55	0·31	8·90	2·29	2·67	0·23	0·29	ND	<0·04	Nil	9·66	—	0·28	96·12	1·34
Agglm.	Flux C	15·70	40·40	8·80	0·96	2·45	15·25	1·32	3·22	0·12	ND	0·09	0·006	Nil	7·40	ND	—	95·71	0·55
	Slag C2	14·40	39·00	7·63	2·17	1·15	10·80	2·43	1·92	0·16	0·03	ND	<0·04	Nil	10·07	—	0·13	89·76	0·57
Agglm.	Flux D	36·20	15·90	0·76	0·63	22·35	12·90	1·34	3·62	0·12	ND	0·056	0·004	Nil	5·55	ND	—	99·63	0·89
	Slag D2	30·07	11·00	0·23	2·40	21·80	12·90	2·74	1·88	0·16	0·03	ND	<0·04	Nil	8·22	—	0·20	91·5	1·18
Agglm.	Flux E	13·90	1·53	2·02	2·41	0·55	0·48	0·38	11·39	c 61	ND	0·041	0·006	Nil	45·20	ND	—	*92·98	2·64
	Slag E3	13·70	<1·50	1·58	5·06	0·40	0·80	3·42	10·40	0·39	0·10	ND	<0·04	Nil	39·04	—	0·13	*92·83	2·44
Agglm.	Flux F	12·8	17·75	0·56	7·63	31·80	1·00	0·76	0·87	0·61	ND	0·049	0·003	0·80	24·04	ND	—	98·67	3·00
	Slag F4	11·8	16·30	0·61	8·69	29·90	1·30	1·62	0·85	0·78	0·10	ND	<0·04	0·21	23·63	—	0·20	94·07	3·13
	Slag F5	12·0	20·80	0·58	8·67	28·10	0·90	0·85	0·95	0·72	0·16	ND	<0·04	0·21	22·60	—	0·25	96·67	2·73
Agglm.	Flux G	36·00	0·48	2·90	25·67	0·05	2·58	0·23	0·10	2·38	ND	0·026	0·004	3·16	22·60	1·45	—	97·57	1·38
	Slag G6	33·60	<1·5	2·90	24·01	0·15	6·90	2·34	0·34	2·65	0·33	ND	<0·04	0·27	21·57	—	0·63	97·09	1·49
Agglm.	Flux H	31·9	0·48	2·42	26·94	0·65	3·72	0·36	0·10	2·99	ND	0·022	0·006	1·80	20·14	1·45	—	92·95	1·58
	Slag H6	30·7	<1·5	3·15	22·48	0·31	8·50	2·11	3·31	2·95	0·26	ND	<0·04	0·13	19·52	—	0·22	95·18	1·64

*Flux E contains 14·45% ZrO_2 *Slag E3 contains 16·50% ZrO_2 ★ IIW (18).

(1) to supply heat to the system by acting as the resistive medium to passage of electric current;

(2) to remove certain impurities from the liquid metal by:
   a) mass transfer across the liquid metal/liquid slag interface
   b) dissolution of inclusions
   c) flotation of particles from the liquid metal;

(3) to isolate the refined product from both the surrounding atmosphere and from direct contact with the cooled mold.

The slags in the submerged arc welding process serve almost identical functions. In welding the arc cavity reactions will provide higher temperatures although the molten flux arc enclosure modifies the arc pattern. In welding, the mold is the molten crater and the difference in density floats the molten slag to the surface where it solidifies.

Mori (22) presents a new scale of basicity in oxide slags. He also suggests that Al_2O_3 and TiO_2 may both act in an amphoteric manner depending upon whether they are added to an acidic or basic slag.

Basic fluxes produce weld metals with low oxygen, silicon, sulphur, and phosphorus contents usually with improved toughness. By expanding on these effects of flux basicity with additions such as zirconium, barium, and titanium oxide for special effects it should be possible to produce acceptable submerged arc weld metal in the HY-130 system. The basic fluxes may have difficult slag removal and poor bead appearance similar to that in the case of basic versus acid coatings for covered electrodes.

A review of the ceramic phase diagrams is useful as a guide in the formulation of submerged arc fluxes. The calcium silicate $CaO\text{-}SiO_2$ system (Figure 8) has been widely used (23). The addition of Al_2O_3 lowers the melting temperature for the binary calcium silicate (Figure 9). Further

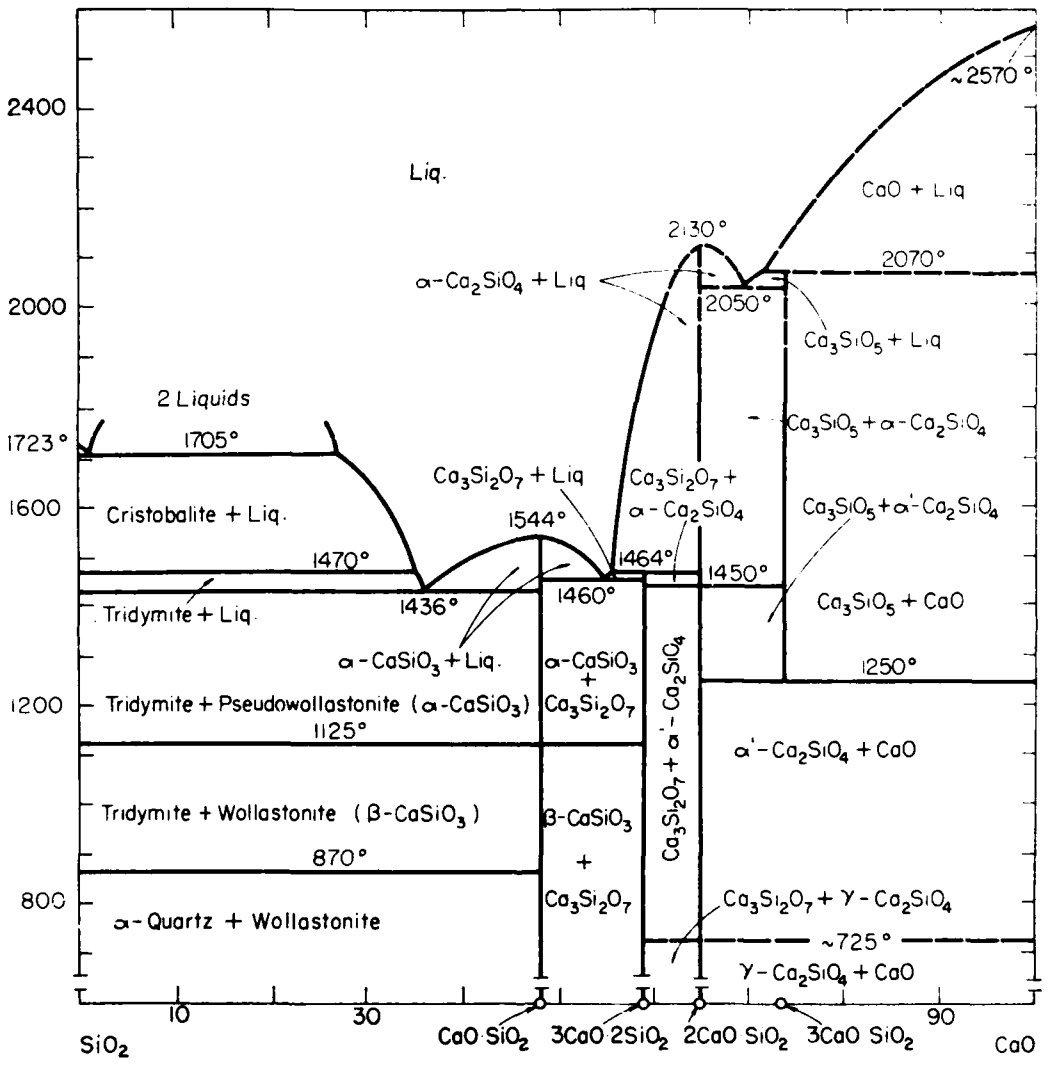

Figure 8. Phase Diagram for $CaO-SiO_2$ System (24). °C

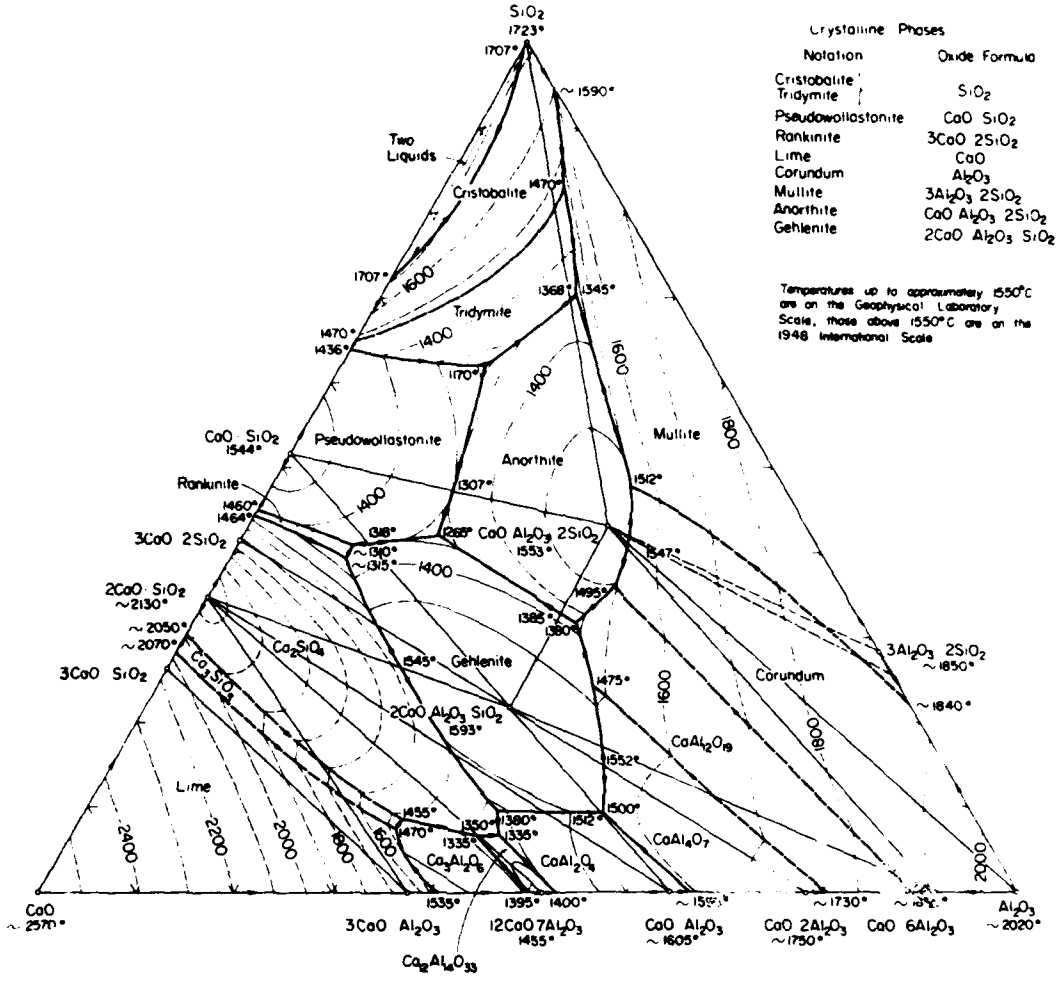

Figure 9. Phase Diagram for $CaO-Al_2O_3-SiO_2$ System (24). °C

modification by the addition of magnesium oxide has been reported (25). In order to improve the basicity many of the manganese and lime silicate fluxes have been converted to the $MgO-SiO_2$ system (Figure 10). The fact that Mg has a lower atomic weight than Ca contributes to a higher basicity for the magnesia composition compared with the lime type. Here again the addition of alumina provides a reduction in the melting temperature (Figure 11). This can be further reduced by the addition of calcium fluoride which also acts as a scavanger, improves electrical stability and decreases the viscosity. Although there are a number of other factors which influence the performance of the higher basicity materials, tests show that as the basicity increases the oxygen content of the weld metal is lowered.

In studies of slag-metal reactions in welding, recognition of the extensive investigations of fluxes in steel-making technology (26), (27), (28), (29) has been helpful. In steel making furnaces there are four phases: gas, slag, metal and a refractory lining. In steel making, owing to the difference between the rates for the various reactions between these phases, only a few of the metallurgical reactions approach equilibrium. The higher temperatures and shorter exposure time in the welding arc modify the slag/metal behavior still further. A more complete description of the welding flux reactions may be obtained if kinetic and physiochemical data are considered in addition to the thermodynamic relationships. In studies of the slag/metal phase in welding the thermodynamic data for oxides and oxide compounds are useful and helpful. As a rule, such an approach makes it possible to obtain plausible results even though actual slags formed from welding fluxes are

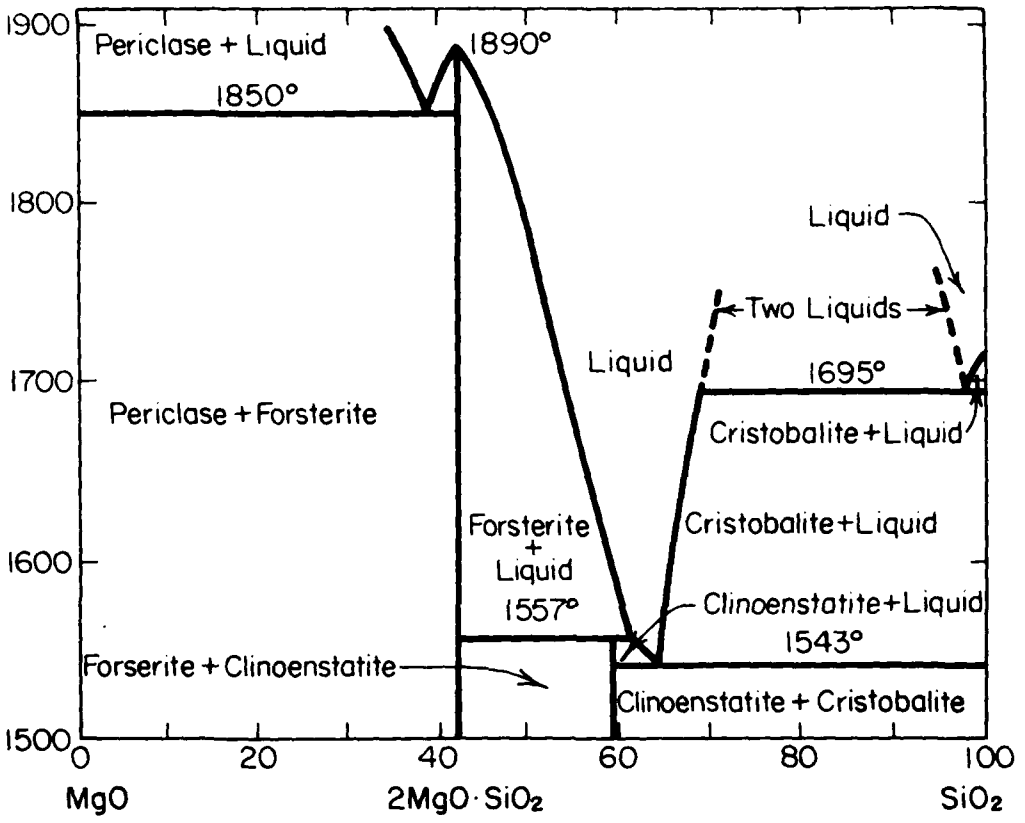

Figure 10. Phase Diagram for $MgO-SiO_2$ System (24). °C

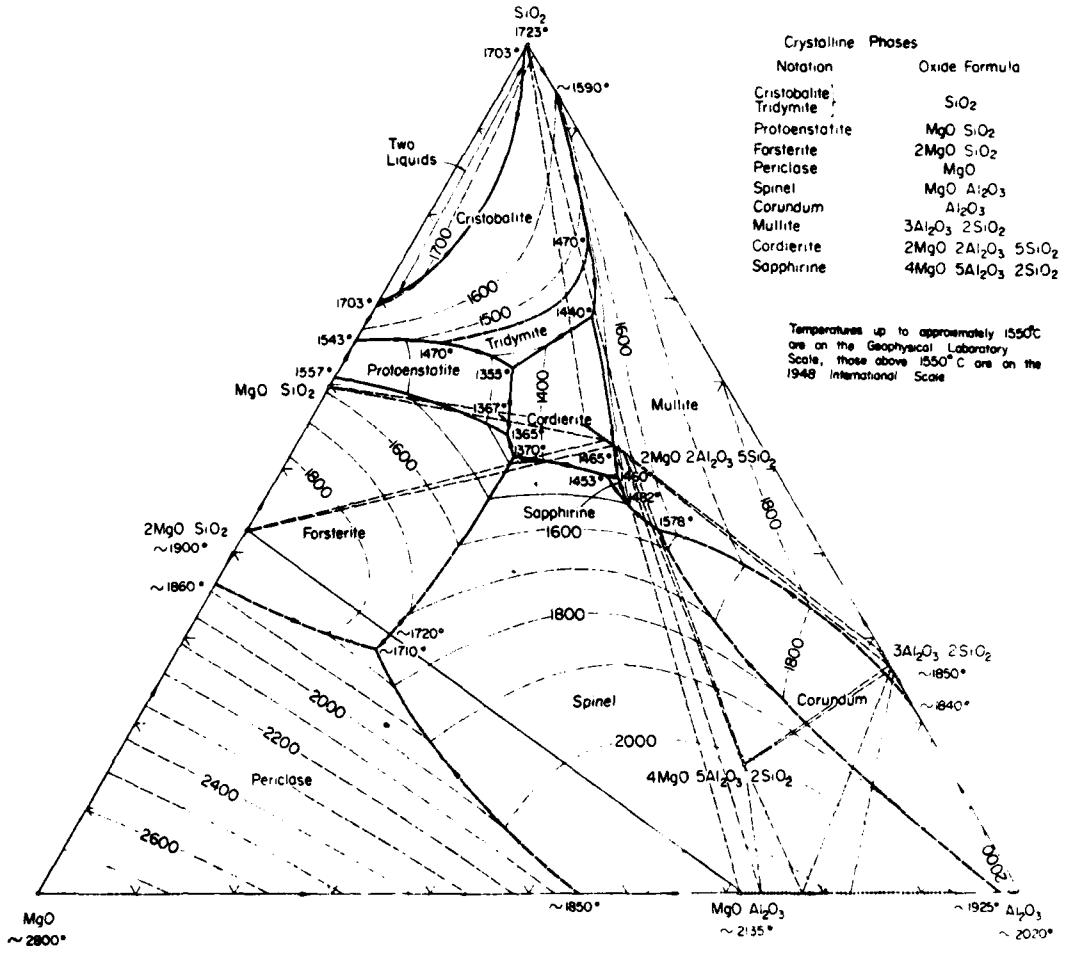

Figure 11. Phase Diagram for $MgO-Al_2O_3-SiO_2$ System (24). °C

complex chemical systems. Progress can be made even though there is no universal neutral welding flux.

Control of Weld Metal Cooling Rates

One of the most important considerations in the selection of welding procedures is the control of the cooling rate of the weld metal and the heat affected zone. In order to investigate the effect of welding technique on weld metal cooling rates, cooling curves have been measured for a wide range of submerged arc welding techniques (30), (32). Temperature time curves can be obtained by plunging a platinum vs platinum 13% rhodium thermocouple into the melted weld pool behind the arc. A typical milli-volt time curve is drawn in Figure 12. A comparison of the cooling rates at 1000°F (538°C) has been found to be useful in comparing the effect of welding techniques. At this temperature the positioning of the thermocouple is not critical since the temperature gradient in the weld area has been reduced. With the higher strength steels this temperature is still above the transformation temperature and hence will not be influenced by the heat of transformation. In heat treating applications, many investigators have used the cooling rate at 1300°F (704°C) as a point of comparison. The cooling curve shown in Figure 12 gives a cooling rate at 1300°F (704°C) which is 1.59 times that at 1000°F (538°C). Data reported by Dorschu et al (30) plotted in Figure 13 shows that the average cooling rate at 1300°F (704°C) is 1.54 times that at 1000°F (538°C). Other investigators show a similar relationship.

Many other investigators have reported cooling rates (31) by giving the time interval for cooling from 800°C (1472°F) to 500 C (932°F). Tests

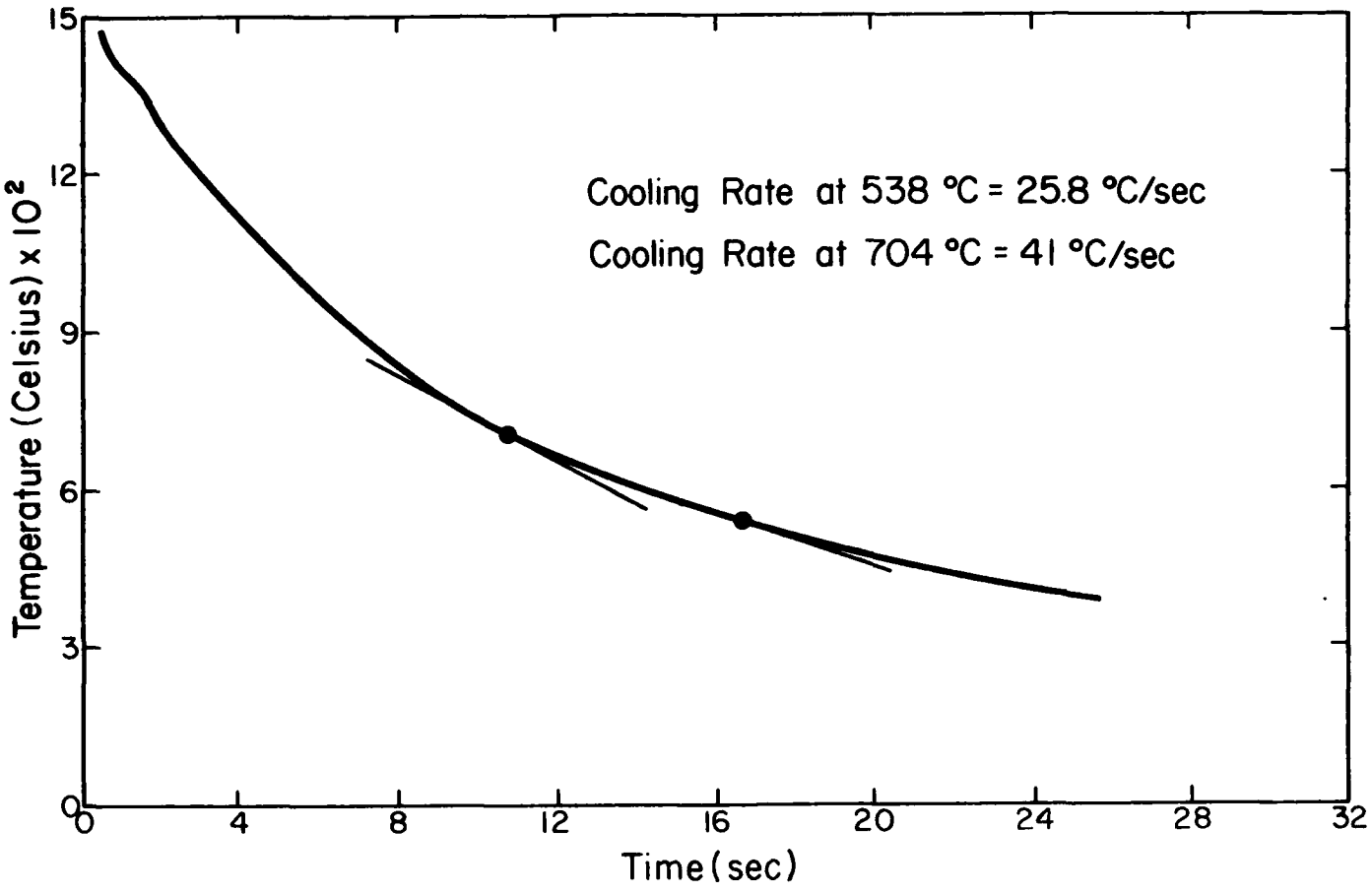

Figure 12. Temperature-Time Curve for Bead Weld on Plate Surface using 304 amperes EP, 24 volt and 9.3 inches per minute travel (32).

plotted in Figure 14 show a linear relationship of the average cooling rate from 800 to 500°C to the cooling rate at 1000 F (538 C).

From a metallurgical standpoint, the weld metal and the heat affected base metal are subjected to a thermal cycle that ranges from that of a relatively slow air cool to a fast water quench. Hence, depending on conditions, the weld metal and heat affected base metal may contain soft, fully hardened or mixtures of soft and hard microstructures. This is true since the thermal history and composition of both the deposited metal and the heat affected zone control the resulting metallographic structure.

For any of the welding processes the volume of molten metal depends on the heat input and the efficiency of using this heat to produce the molten metal. Various degrees of success have been reported by investigators (3), (32) using the thermal input for predicting cooling rates and subsequent mechanical properties of welding. One of the major difficulties in this approach is that of precisely indicating the effective energy which is transferred from the heat source to the plate. Modern welding processes with available techniques utilize 30 to 80% of the energy input to produce molten metal (33). The exact relationship between welding technique and the efficiency of energy utilization depends on the specific welding technique used for depositing the weld metal and is not a constant even for given welding process. The weld metal in a single pass contains the intimate mixture of molten weld metal and fused base metal. The heat is dissipated mainly into a thermal-conducting base metal during solidification and cooling of the assembly to a uniform temperature. A measure of the effective heat source for weld metal cooling

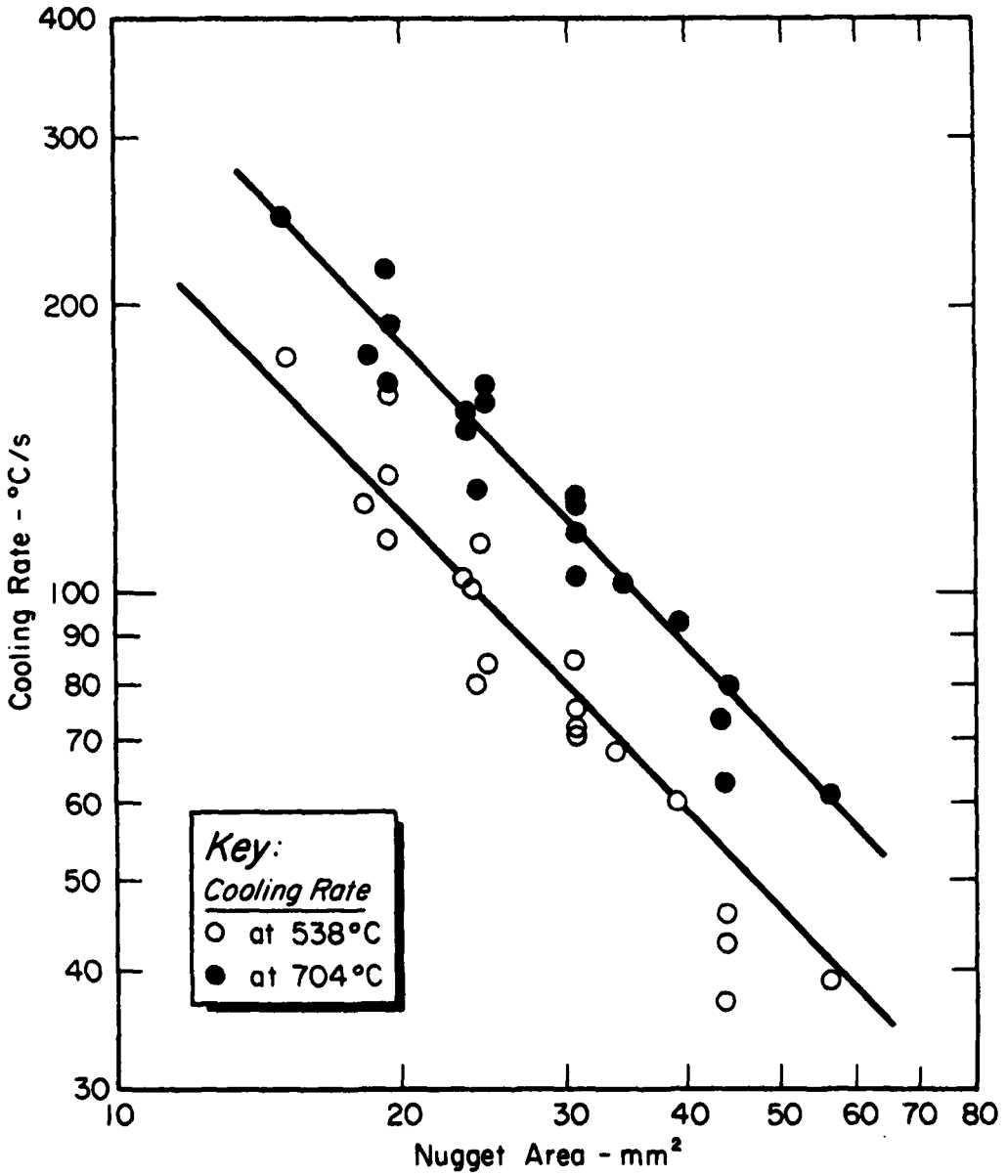

Figure 13. A comparison of the Influence of Nugget Area on the Cooling Rate at 538°C (1000°F) and 704°C (1300°F). (30)

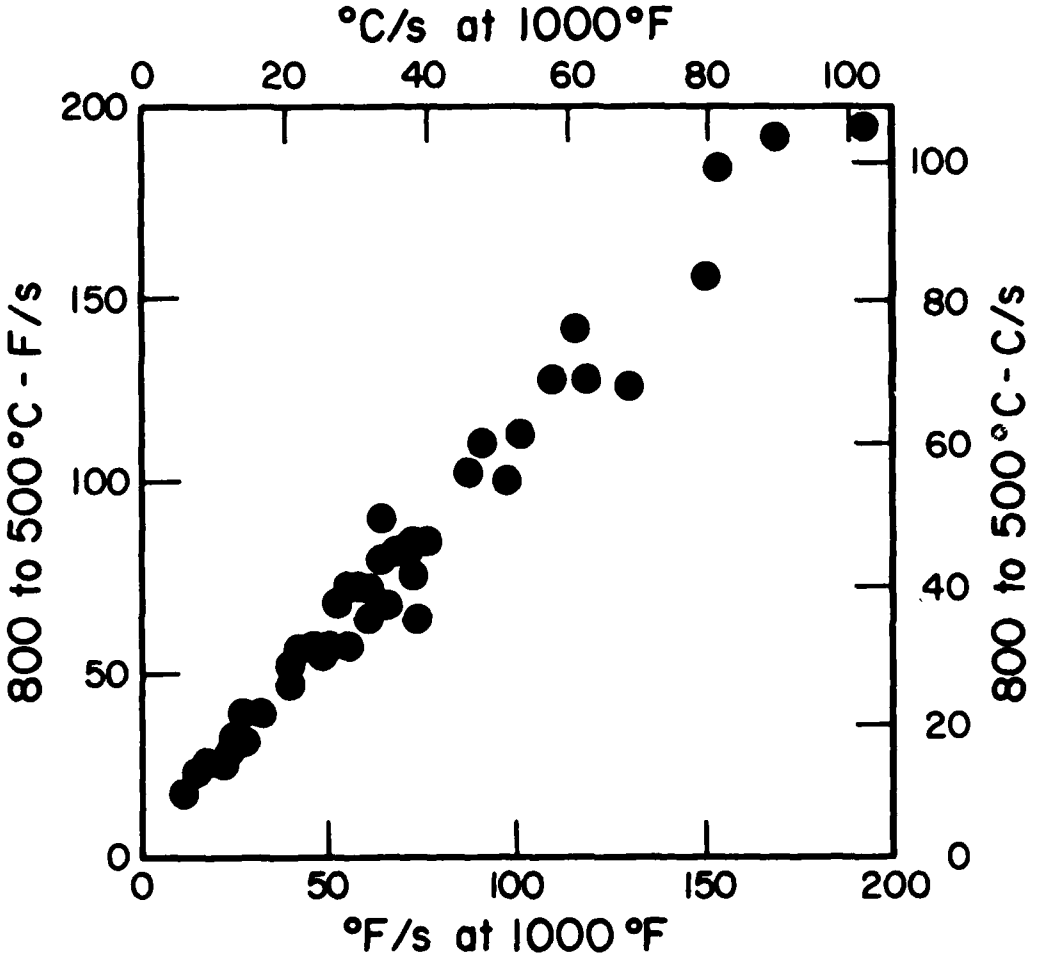

Figure 14. Comparison of Cooling Rate as Measured by the Average Cooling Rate from 800 to 500°C (1472 to 932°F) and the tangent at 1000°F (538°C).

rates is the calorific heat content of the molten weld metal. The heat content is proportional to the weld bead cross sectional area (weld nugget area) (Figure 15). The weld nugget area represents the amount of metal which has been heated to the molten state; the dissipation of this heat controls the cooling in the weld zone.

For a specific welded section, the cooling rate depends on the heat in the molten metal in the bead weld. The greatest portion of this heat is transmitted to the base metal immediately after the weld bead is produced. The cooling rate associated with the weld nugget depends on the heat content of the molten weld metal and the mass and ambient temperature of the base metal.

It is recognized that in many discussions of the changes of cooling rates caused by variations in welding conditions, the effect is assumed to be a linear function of the energy input and the time per unit length. This assumption is reasonably valid for the energy inputs up to 50,000 joules per inch (2,000 joules per mm) with low currents and slow travel speeds used in manual operations (Figure 16). However as the current and the rate of travel increases for a given energy input the melting efficiency of the welding process improves. Hence the cooling rate will be governed by the nugget area or the cross sectional area of the weld bead and to a lesser extent by the energy input per unit length of weld.

The cooling rate in the weld zone depends mainly on three variables:

1. the rate of heat input as measured by the nugget area,
2. the base metal and temperature, and
3. the section thickness and the joint dimensions.

The cooling rate associated with a weld bead deposited in a single

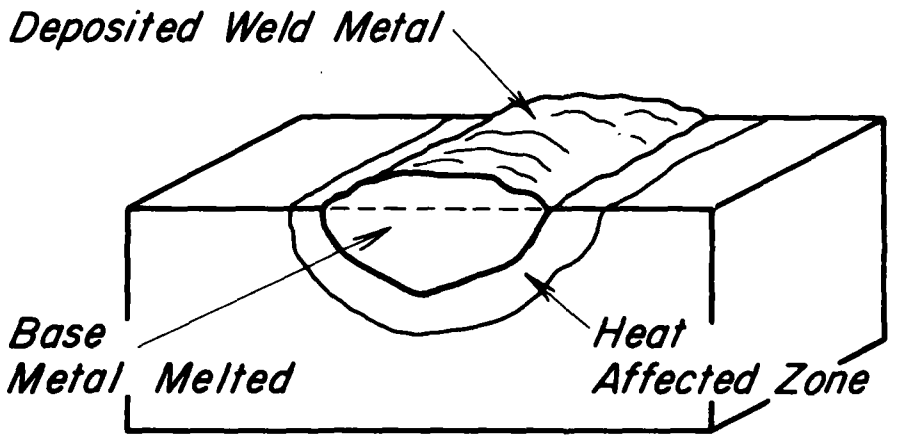

Figure 15. The Cross-Sectional Area of a Bead Weld which Includes Base and Deposited Metal is the Weld Nugget Area.

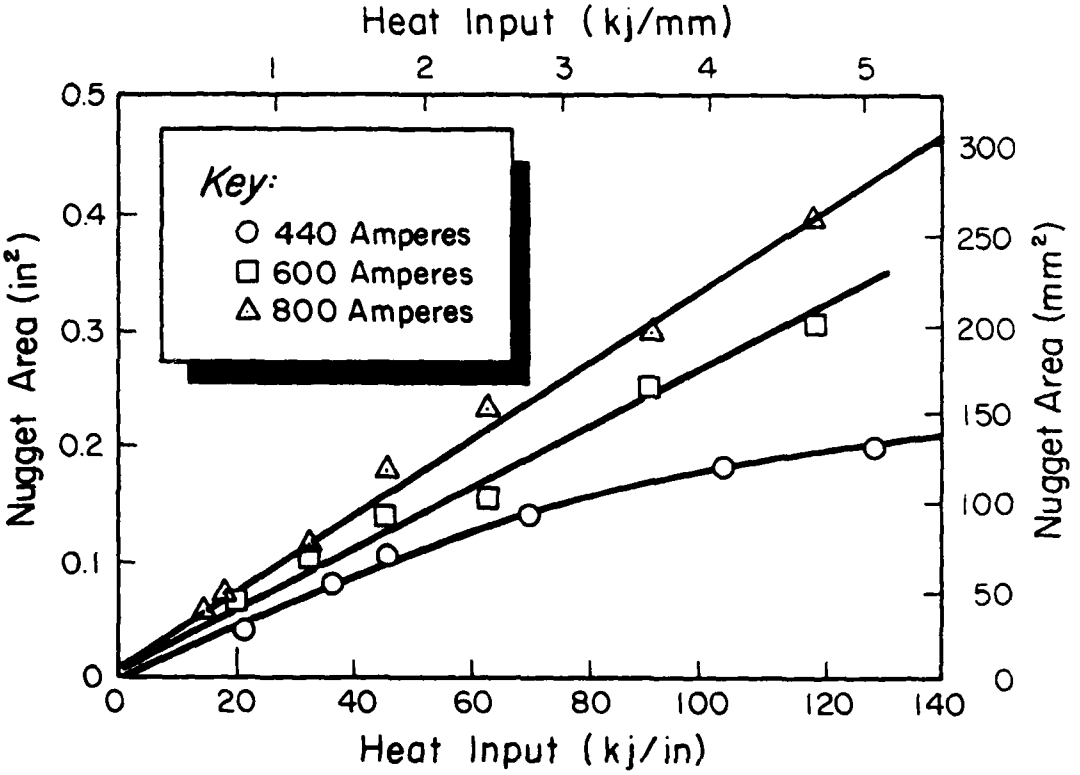

Figure 16. Effect of Heat Input on Nugget Area.

pass with a specified welding technique has been reported by numerous investigators (34),(35). On log-log graph paper (Figure 17), the relationship between the nugget area (na) and weld cooling rate at 1000°F is a straight line described by the equation:

$$^{\circ}F/s = \frac{2,6}{na^{1.119}} \qquad \text{for na in square inches}$$

$$\text{or } ^{\circ}C/s = \frac{2012}{na^{1.119}} \qquad \text{for na in square millimeters}$$

Preheating and high heat input promote slower cooling while heavy sections encourage faster cooling. With a constant energy input the nugget area or the cross sectional area of a bead weld increases with increasing speed of travel. Sufficient empirical data have been accumulated (2), (36) so that the effect of welding parameters on the nugget area of the bead weld can be predicted. The following equation has been tested in many arc welding applications with the covered electrode, submerged arc and some gas shielded metal arc processes;

$$na(in^2) = 1,122 \times 10^{-7} \frac{A^{1.55}}{S_{i/min}^{0.903}}$$

where $na(in^2)$ = Nugget area, square inches

A = Welding Current, amperes

S = Speed of travel, inches per minute

$$\text{or } na(mm^2) = 33,312 \times 10^{-6} \frac{A^{1.55}}{S_{mm/s}^{0.903}}$$

where $na(mm^2)$ = Nugget area, square millimeters

A = Welding current, amperes

S = Speed of travel, millimeters per second.

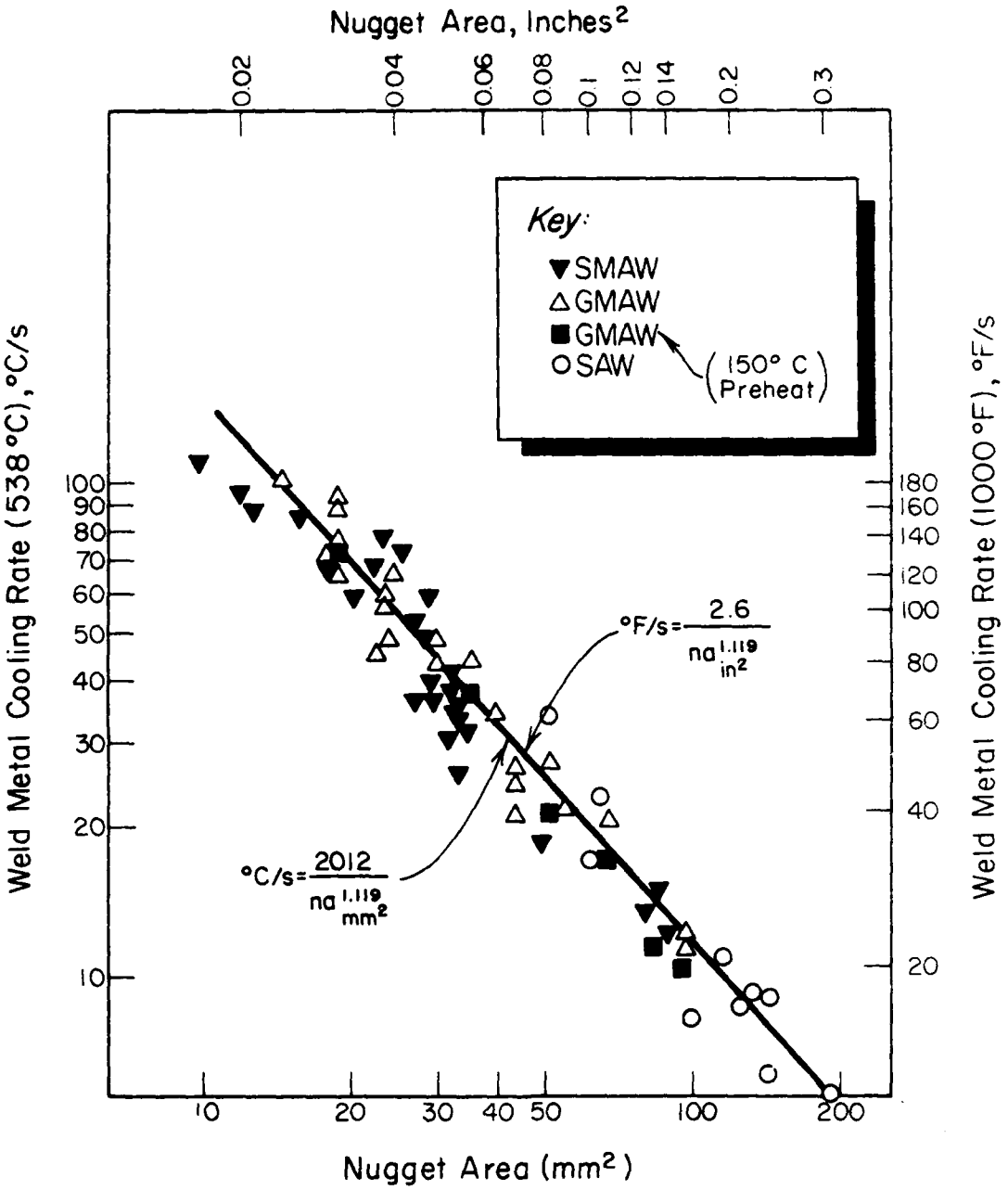

Figure 17. Effect of Nugget Area on Weld Metal Cooling Rate at 538 C (1000 F).

Although these calculations may be a little cumbersome, even a simple handheld scientific calculator is adequate for quickly calculating the nugget area. It can also be noted that for a given energy input the nugget area increases with the current and speed of travel. The effect of increased current and travel speed on nugget area is shown in Figure 16. A further indication of the effect of input on cooling rates at various current levels can be shown in Figure 18. Here a cooling rate of 34° F (19°C) for a 0.10 in^2 (64.5 mm^2) nugget area can be obtained using 30 to 60 kj/in heat input with currents of 1000 to 200 amp.

EXPERIMENTAL PROCEDURES

The fluxes used in this research program were produced by fusing raw materials in a graphite lined furnace. Fused fluxes were chosen for this study for several reasons. First they are considered less hygroscopic and would not present a large hydrogen embrittlement problem when used with the high strength steels, as opposed to some bonded or agglommerated fluxes. Second the chemical homogeneity of the crushed flux would remain constant from fine to coarse particles.

Raw Materials

The raw materials used in this investigation were divided into three main categories:

Level I - These are materials in their semi-refined form (i.e., better than as-mined)

Level II - Raw materials in refined form as commercially available

Level III - Reagant grade chemicals.

The Level I materials were in the range of 80-90% purity, for example, the magnesia raw material contained 85% MgO with the balance

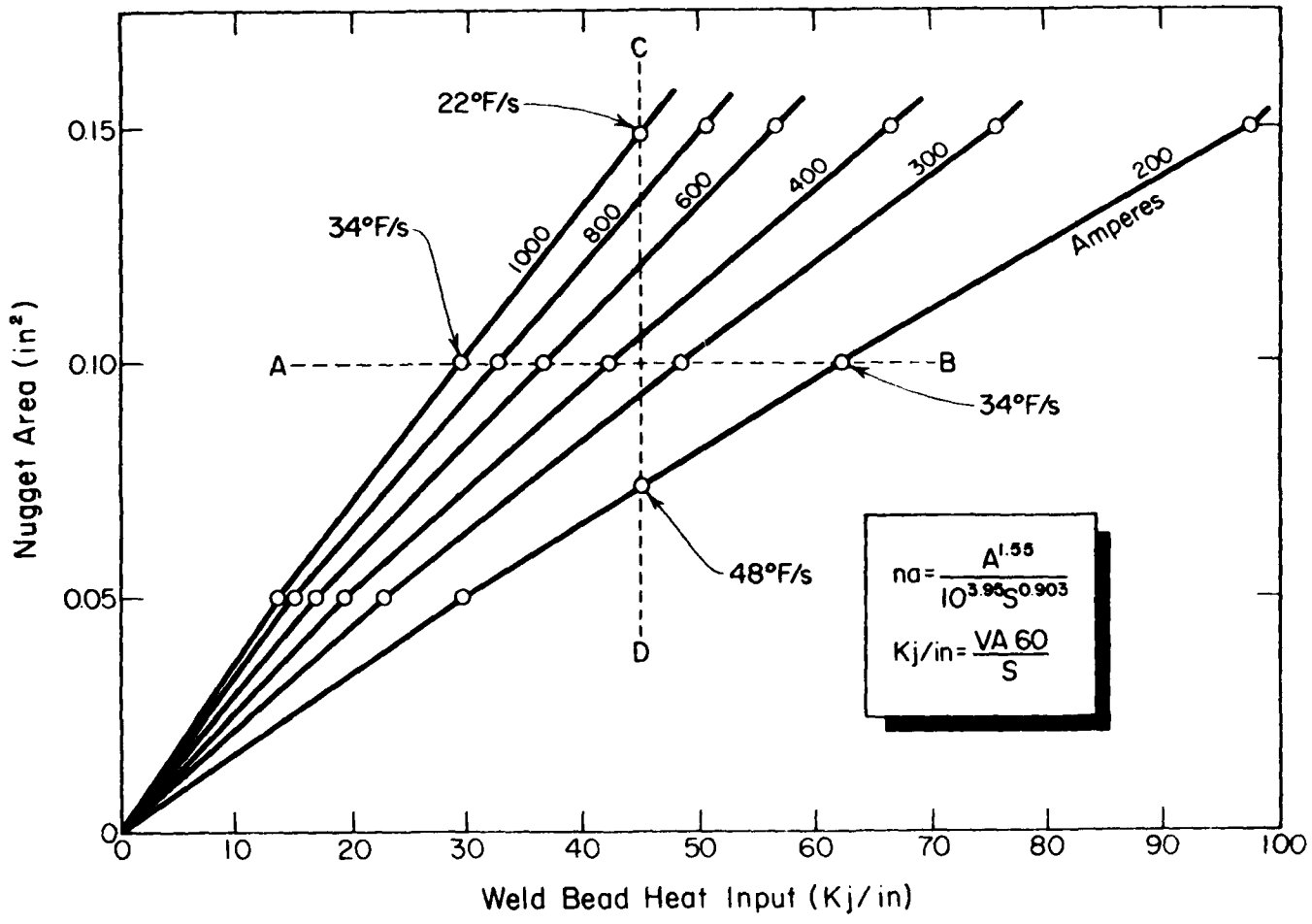

Figure 18. The Effect of Heat Input and Welding Current on the Relationship of Nugget Area to Cooling Rate. (Note the change in heat input as the current is decreased from 1000 to 200 amperes for a 0.10 in^2 nugget area).

consisting of earth trace materials. Level II materials were typically in the range of 95-98% pure constituents with the balance the sum of trace materials. Level III materials of reagent grade contained 99+% pure major element.

Flux Formulation and Preparation

The fluxes which were prepared varied in composition but were all of the magnesia-alumina-silica family. Magnesium oxide was used to replace calcium oxide and calcium carbonate as the primary basic component. Due to the lower molecular weight of MgO as compared to CaO or $CaCO_3$ a higher level of basicity can be realized with the use of MgO in a given percentage in the formulation.

The method of determining basicity of the experimental fluxes used in this investigation is based on the following equation:

$$\text{Basicity} = \frac{\text{Base}}{\text{Acid}} = \frac{MgO + CaO + BaO + \frac{1}{2}Al_2O_3}{SiO_2 + \frac{1}{2}Al_2O_3 + TiO_2 + ZrO_2}$$

Each compound is added to the numerator or denominator as weight percent of the compound ÷ molecular weight. As an example, the base/acid ratio of a typical flux is calculated as follows:

Flux Composition	Weight Percent	÷ Molecular Weight	= Ratio
MgO	26.3	40.3	0.652
Al_2O_3	22.0	101.96	0.216
SiO_2	16.0	60.09	0.266
TiO_2	1.5	79.9	0.019
ZrO_2	4.2	123.22	0.034
CaF_2	25.0	--	--
$CaCO_3 \rightarrow CaO$	5.0	56.08	0.050
TOTAL	100.0		

$$\text{Basicity} = \frac{\text{Base}}{\text{Acid}} = \frac{0.652 + \frac{1}{2}(0.216) + 0.050}{0.266 + \frac{1}{2}(0.216) + 0.019 + 0.034} = 1.89$$

The flux is considered basic.

Previous experiments of Jackson (37) suggested the choice of MgO-Al_2O_3-SiO_2 compositions suitable for welding. The range of flux component compositions studied in the present investigation is shown in Table 4.

Other compounds which were added to the fluxes in some heats in order to study specific effects were NiO, Cr_2O_3, and $BaCO_3$.

The flux compositions were fused in a graphite crucible using an open arc to initiate the melting followed by resistance heating with a submerged electrode to complete the fusion in an electo slag manner. Approximately one hundred heats ranging from 4 to 20 pounds each were melted using the compositions shown in Table 5. In a number of cases several heats were made of a given composition in order to provide sufficient flux for testing. In the smaller heats which showed greater energy losses, up to 1.4 kwh electrical energy was required per pound of flux. In the 20 pound heats this was reduced to 0.8 kwh per pound. After chill casting the molten flux on a steel plate the sample was collected and crushed to pass a 20-mesh screen.

In Table 6, the values shown for $CaCO_3$, with the exception of VHP-XX are amounts added after fusing. The same procedure was also used for the addition of $BaCO_3$ in VHP-II-B and VHP-XXIV-BC, as well as with the addition of NiO and Cr_2O_3 in VHP-XI, VHP-XII, VHP-XIII, and VHP-XIV. The basicity for these fluxes was calculated based on charge formulation. These basicity values of the as-mixed fluxes prior to fusing were used as the reference throughout this investigation. Although this procedure

Table 4

Range of Flux Composition Compounds Studied.

Compound	Weight Percent
MgO	20 - 40
Al_2O_3	10 - 25
SiO_2	5 - 25
CaF_2	10 - 50
CaO	30 - 50
$CaCO_3$	5 - 10
TiO_2	1 - 10
ZrO_2	4 - 15

Field Designation	MgO	SiO_2	Al_2O_3	CaF_2	$CaCO_3$	TiO_2	ZrO_2	NiO	Cr_2O_3	MnO	$BaCO_3$	Base/Acid Ratio	Weld Metal O_2 - ppm
EHP-I	29.1	17.5	24.1	24.7	--	--	4.6	--	--	--	--	1.89	--
HP-II	29.1	17.5	24.1	24.7	--	--	4.6	--	--	--	--	1.89	313
VHP-I	29.1	17.5	24.1	24.7	--	--	4.6	--	--	--	--	1.89	329
VHP-III	22.3	36.1	16.6	25.0	--	--	--	--	--	--	--	0.93	623
VHP-IV	36.2	12.5	16.6	28.3	5.4	1.0	--	--	--	--	--	3.43	265
VHP-V	27.45	16.70	22.96	26.10	5.20	1.57	--	--	--	--	--	2.07	260
VHP-VII	36.21	16.64	17.14	27.11	2.90	--	--	--	--	--	--	2.80	174
VHP-VI	36.6	12.6	16.8	28.6	5.5	--	--	--	--	--	--	3.59	153
VHP-II	26.3	16.0	22.0	25.0	5.0	1.5	4.2	--	--	--	--	1.78	231
VHP-VI-Al	36.7	13.3	17.8	30.2	--	--	--	--	--	--	--	1.91	144
VHP-II-B	26.3	16.0	22.0	25.0	--	1.5	4.2	--	--	--	5.0	1.84	124
VHP-VIII	26.3	10.0	22.0	25.0	--	3.5	10.2	--	--	--	--	1.91	180
VHP-IX	26.3	5.0	22.0	25.0	--	5.0	16.7	--	--	--	--	1.95	110
VHP-X	26.3	10.0	22.0	25.0	--	6.5	10.2	--	--	--	--	1.74	170
VHP-XI	26.3	16.0	22.0	25.0	5.0	1.5	4.2	5.0	--	--	--	2.10	258
VHP-XII	26.3	16.0	22.0	25.0	5.0	1.5	4.2	--	5.0	--	--	1.76	275
VHP-XIII	36.6	16.8	12.6	28.6	5.5	--	--	5.0	--	--	--	3.19	211
VHP-XIV	36.6	16.8	12.6	28.6	5.5	--	--	--	5.0	--	--	2.73	324
EHP-VI	36.6	12.6	16.8	28.6	5.5	--	--	--	--	--	--	3.57	80
VHP-XVI	36.0	15.0	14.0	35.0	--	0.5	--	--	--	--	--	2.98	205
VHP-XVII	30.0	10.0	10.0	50.0	--	--	--	--	--	--	--	3.69	121
VHP-XVIII	32.2	14.87	11.09	36.6	5.5	--	--	4.4	--	--	--	3.01	173
VHP-XIX	23.9	14.56	20.02	35.0	5.29	1.36	3.8	--	4.55	--	--	1.78	263
VHP-XX	20	--	16.2	30.0	30.0	1.40	--	--	--	--	--	9.10	84
VHP-XXII	24.85	16.0	20.79	30.0	5.0	1.42	3.97	--	--	3.42	--	2.12	204
VHP-XXIII	38.0	26.0	26.0	10.0	--	--	--	--	--	--	--	1.94	480
VHP-XXIV	36.0	24.75	24.75	15.0	--	--	--	--	--	--	--	1.90	360
VHP-XXV	32.5	22.52	22.52	25.0	--	--	--	--	--	--	--	1.89	185
VHP-XXIV-BC1	36.0	24.5	24.5	15.0	--	--	--	--	--	--	5.0	1.97	185
VHP-XXIV-BC2	36.0	24.5	24.5	15.0	--	--	--	--	--	--	10.0	2.02	181

Table 5. Chemical composition of Experimental Fluxes in Percent by Weight.

may introduce error, it was based on check chemical analyses which indicated that in most cases only minor amounts of the flux constituents in these heats were lost. A more realistic approach would be a chemical analyses of the slag collected from the welding tests. In accurate determinations for international studies a reference chemical standard sample for serious investigators should be available.

Chemical Analysis Pads

Chemical analysis pads were prepared in accordance with American Welding Society specification, AWS A5.5-69 Section 2 Appendix A. The pads were constructed with about 20 passes in a pyramid fashion 5 layers high. A cross section of a typical pad is shown in Figure 19. Samples for chemical analysis were extracted ¼ inch below the top surface of the last weld layer. Deposition of pads were made using 400 amp, electrode positive; 30 volts and 10 to 12.5 inches per minute travel. The base material used for all of the pads was 7/8 inch thick HY-130 with a typical chemical composition shown in Table 6. The composition of the filler metal is also given in Table 6.

The base metal was cut into 6 inch . 4 inch x 7/8 inch pads; a threaded stud fastener was welded for a ground connection on each plate. The filler wire used was 1/8 inch diameter. Chemical analyses for silicon, oxygen and nitrogen which were determined by a testing laboratory are given in Table 7. The oxygen contents ranged from 0.0080 to 0.0623% (80 to 623 parts per million). A plot of the basicity (calculated from the chemical composition given in Table 5) against weld metal oxygen content is given in Figure 20. These data show that the oxygen content of the weld metal decreases as the basicity of the flux increases. The

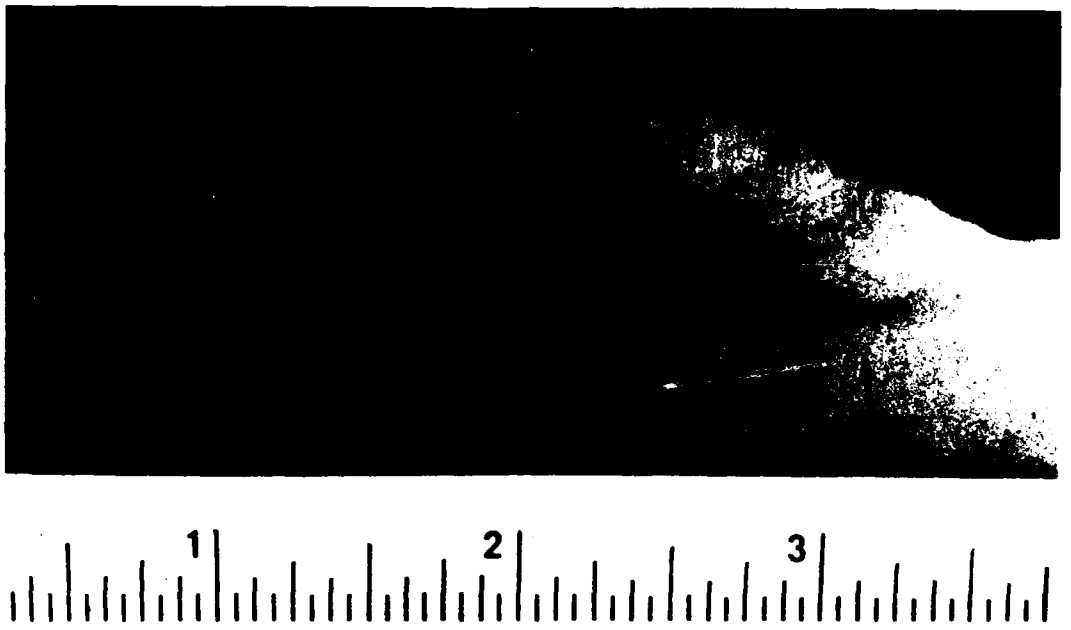

Figure 19. Macrophotograph of Cross Section of Typical Chemical Analysis Pad. Etchant: 2% Nital.

Table 6

Chemical Composition of HY-130 Plate and 140 Filler Metal.

Element	Plate HY-130	Filler Metal 140
C	0.12 %	0.12%
Mn	0.6 - 0.9	1.57
Si	0.2 - 0.35	0.37
S	0.010	0.010
P	0.010	0.006
Ni	4.75 - 5.25	2.90
Cr	0.40 - 0.70	0.70
Mo	0.30 - 0.65	0.90
V	0.05 - 0.10	--
Ti	0.02 residual	--
Cu	0.025 residual	--
O	---	0.0016
N	---	0.0042

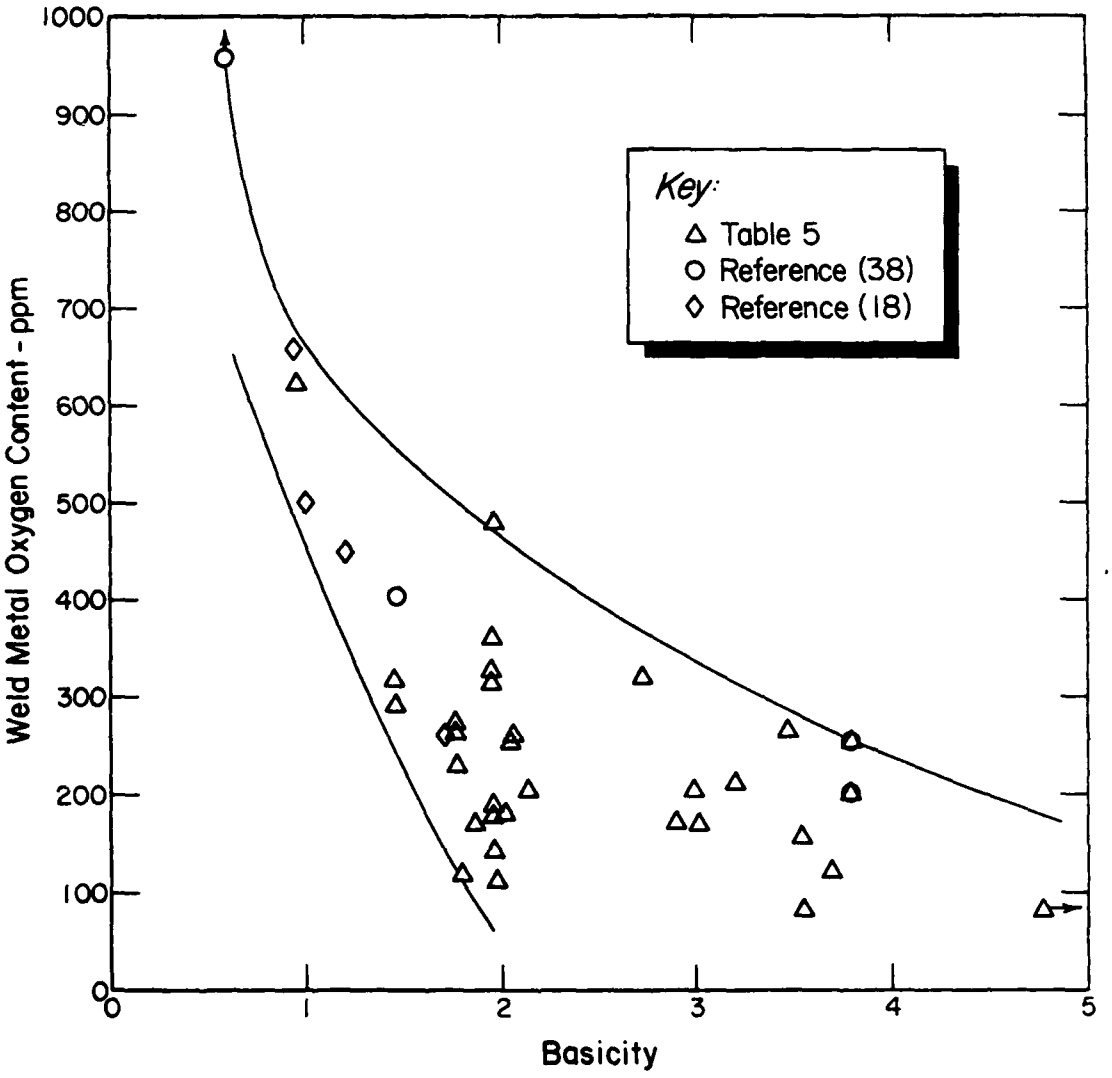

Figure 20. Influence of Basicity of the Welding Flux on the Oxygen Content of the Weld Metal in Multi Pass Pads.

wide scatter of the data indicates that other factors in addition to basicity, control the oxygen content of the weld metal. A review of the results shown in Tables 7 and 8 point to several factors which reduce the weld metal oxygen content. As expected, basicity is a major factor as shown by comparing the results with flux VHP-III and flux VHP-XX; the basicity increased from 0.93 to 9.10 with a decrease of oxygen in the weld metal from 623 to 84 ppm. A second factor which influences the oxygen content is the scavenging action of calcium fluoride. Increasing the CaF_2 content from 10 to 24% (maintaining the basicity at 1.9) reduced the oxygen content from 480 to 185 ppm. A further increase in the CaF_2 to 50% with an increase in basicity to 3.69 reduced the oxygen content to 121 ppm. One of composition factors which depended upon the free energy of formation was the effect of using zirconium oxide in the formulation of the flux. With an increase in ZrO_2 content of 4 to 16% in fluxes VHP-XI and VHP-IX the oxygen content was reduced from 258 to 110 ppm. In a single test, using reagent quality of raw materials, the oxygen content was reduced in VHP-VI compared with EHP-VI from 153 to 80 ppm. Other observations from supplementary tests are given in Table 8. Three pads were made using flux VHP-XXII and voltages of 25, 30 and 35. As the voltage increases the ratio of fused flux to weld metal increases although weld metal oxygen content remained at about the same level. In another series of tests shown in Table 8, the addition of deoxidisers in powder form to the weld zone did not significantly influence the oxygen content of the weld metal. The flux composition in these tests is a controlling factor in the resulting oxygen content of the weld metal.

Chemical Pad Weld Designation	Flux Used	Slag Removal	Bead Appearance	Bead Contour	O (%)	Si (%)	N (%)
1S	A*	--	--	--	0.0292	0.39	--
2S	B	--	--	--	0.0218	0.30	--
3S	C	--	--	--	0.0194	0.28	--
4S	C	--	--	--	0.0200	0.29	--
5S	B	--	--	--	0.0217	0.33	--
6S	A	--	--	--	0.0320	0.32	--
7S	HP-II	--	--	--	0.0313	0.65	--
13S	VHP-I	Good	Good	Convex	0.0329	0.63	0.0059
14S	VHP-II	Fair	Shards	Convex	0.0260	0.50	0.0046
15S	VHP-IV	Fair	Shards	Convex	0.0265	0.29	0.0041
16S	VHP-III	Good	Fair	Convex	0.0623	1.03	0.0112
17S	VHP-V	Poor	Shards	Convex	0.0260	0.58	0.0045
19S	VHP-VI	Good	Good	Convex	0.0153	0.33	0.0055
20S	VHP-II	Poor	Shards	Flat	0.0231	0.58	0.0042
22S	VHP-VI-Al	Good	Good	Convex	0.0144	1.92	0.0049
23S	VHP-II-B	Poor	Shards	Convex	0.0124	0.31	0.0037
24S	VHP-VII	Fair	Shards	Flat	0.0174	0.41	0.0040
25S	VHP-VI	Good	Good	Convex	0.0168	0.47	0.0040
28S	VHP-VIII	Poor	Shards	Convex	0.018	0.73	--
29S	VHP-IX	Poor	Shards	Convex	0.011	0.74	--
30S	VHP-X	Fair	Shards	Convex	0.017	0.63	--

* Commercial Fluxes.

Table 7. Chemical Analysis Pad Results.

Table 7 (continued)

Chemical Pad Weld Designation	Flux Used	Slag Removal	Bead Appearance	Bead Contour	O (%)	Si (%)	N (%)
31S	VHP-XI	Fair	Pock Marks	Convex	0.0258	0.46	--
32S	VHP-XII	Fair	Pock Marks	Convex	0.0275	0.35	--
33S	VHP-XIII	Poor	Pock Marks	Convex	0.0211	0.36	--
34S	VHP-XIV	Fair	Pock Marks	Convex	0.0324	0.20	--
35S	VHP-XV	Good	Good	Convex	0.0268	0.45	--
36S	EHP-VI	Excellent	Shards	Convex	0.0080	0.51	0.0037
37S	VHP-XVI	Excellent	Shards	Convex	0.0205	0.53	0.0063
38S	VHP-XVII	Good	Shards	Convex	0.0121	0.45	0.0048
39S	VHP-XVIII**	Poor	Fair	Convex	0.0173	0.50	0.0034
40S	VHP-XIX	Good	Shards	Convex	0.0263	0.25	0.0036
41S	VHP-XX	Good	Shards	Convex	0.0084	0.21	0.0045
43S	VHP-XXII	Excellent	Shards	Convex	0.0221	0.55	0.0034
44S	VHP-XXII	Good	Pock Marks	Convex	0.0204	0.47	0.0041
45S	VHP-XXII	Good	Pock Marks	Convex	0.0267	0.50	0.0042
46S	VHP-XXIII	Excellent	Good	Convex	0.0480	0.70	0.0083
47S	VHP-XXIV	Excellent	Good	Convex	0.0360	0.69	0.0062
48S	VHP-XXV	Excellent	Good	Convex	0.0365	0.59	0.0051
49S	VHP-XV-5% $BaCO_3$	Good	Shards	Convex	0.0185	0.70	0.0067
50S	VHP-XV-10% $BaCO_3$	Good	Shards	Convex	0.0181	0.36	0.0049

** Weld metal contained 4.89% Ni.

A. Effect of Basicity.

Flux	Basicity	Oxygen - ppm
VHP-III	.93	623
VHP-XX	9.10	84

B. Effect of Calcium Fluoride Content.

Flux	Basicity	CaF_2	Oxygen - ppm
XXIII	1.94	10%	480
XXIV	1.90	15%	360
XXV	1.89	24%	185
XVII	3.69	50%	121

C. Effect of Zirconium Oxide Content.

Flux	Basicity	ZrO_2	Oxygen - ppm
XI	2.10	4.2	258
XII	1.76	4.2	275
XIX	1.78	3.8	263
X	1.74	10.2	170
VIII	1.91	10.2	180
IX	1.95	16.7	110

D. Effect of Purity.

Flux	Basicity	ZrO_2	Oxygen - ppm
VHP-VI	3.59	28.6	153
EHP-VI	3.57	28.6	80

E. Effect of Voltage.

Flux	Basicity	ZrO_2	Oxygen - ppm
XXII 25 volts	2.12	4.0	221
XXII 30 volts	2.12	4.0	204
XXII 35 volts	2.12	4.0	267

Table 8. Summary of Chemical Analyses Pad Results.

Table 8 (continued).

F. Effect of Deoxidizers (38) (39)(40).

Flux	Basicity	Deoxidizer Addition	Oxygen Content ppm
D-(CaO-TiO_2-SiO_2)(38)	0.60	none	1612
		2.5% FeSi	1735
		5% FeSi	1556
	Average		1634
A-(CaO-SiO_2)(38)	1.42	none	349
		2.5% FeSi	502
		5% FeSi	445
		10% FeSi	382
		5% Si	325
		5% Mn	347
		10% FeMnSi	445
	Average		401
(CaO-Al_2O_3)(39)	3.08	none	148
		0.4% Zr	130
		1.0% Zr	120
		1.4% Zr	105
		0.3% FeV	130
		0.7% FeV	120
		1.0% FeV	110
		0.4% MoTi	110
		0.4% Ti, 0.1 B_2O_3	100
(CaO-SiO_2)(40)			
slag CaO/SiO_2	0.15	none	2600
$NCaO/NSiO_2$	0.17	8% FeSi	1900
		16% FeSi	1700
		32% FeSi	1400

Table 8 (continued).

slag CaO/SiO_2	.79	none	1200
$NCaO/NSiO_2$	.84	2% FeSi	1000
		4% FeSi	900
		16% FeSi	500
		32% FeSi	500

Mechanical Property Tests

Mechanical property weldments were fabricated with HY-130 plate. The base plate and filler metal used for these plates were the same as used for the chemical analysis pads. The test plates were flame cut and the bevel cleaned up by grinding. Test plate dimensions and joint design are shown in Figure 21. A preheat, interpass and postheat temperature of 250°F was maintained by use of resistance heaters. A welding technique with parameters chosen to yield a nugget area of 0.10 in^2 and a heat input of approximately 50 kilojoules per linear inch was used. This is in agreement with previous data, shown in Figure 22, using three processes to weld HY-130 plate.

Uwer (42) states that the temperature cycles occurring in the weld region during welding determine the mechanical properties in the heat affected zone of welded joints. The influence of the welding conditions on the mechanical properties of shielded metal arc, gas metal arc and submerged arc welding can be controlled by the cooling rate. Uwer reports the cooling rate as the time which is required for the weld bead to pass through the temperature range from 800 to 500°C. As shown in Figure 14, a linear relation exists between the cooling time from 800 to 500°C (1472 to 932°F) and the cooling rate or slope of the tangent at 1000°F (538°C). The molten metal in the weld bead which is measured by the nugget area is a controlling factor in the cooling rate studies. A current of 400 to 410 amperes with a voltage of 28 to 31 and a travel of 14 to 15 inches per minute was used. Twelve to sixteen passes were needed to complete the joint. After welding was completed, the postheat temperature of 250°F was maintained for 24 hours. Plates for test were sectioned and specimens for mechanical testing were prepared. Testing

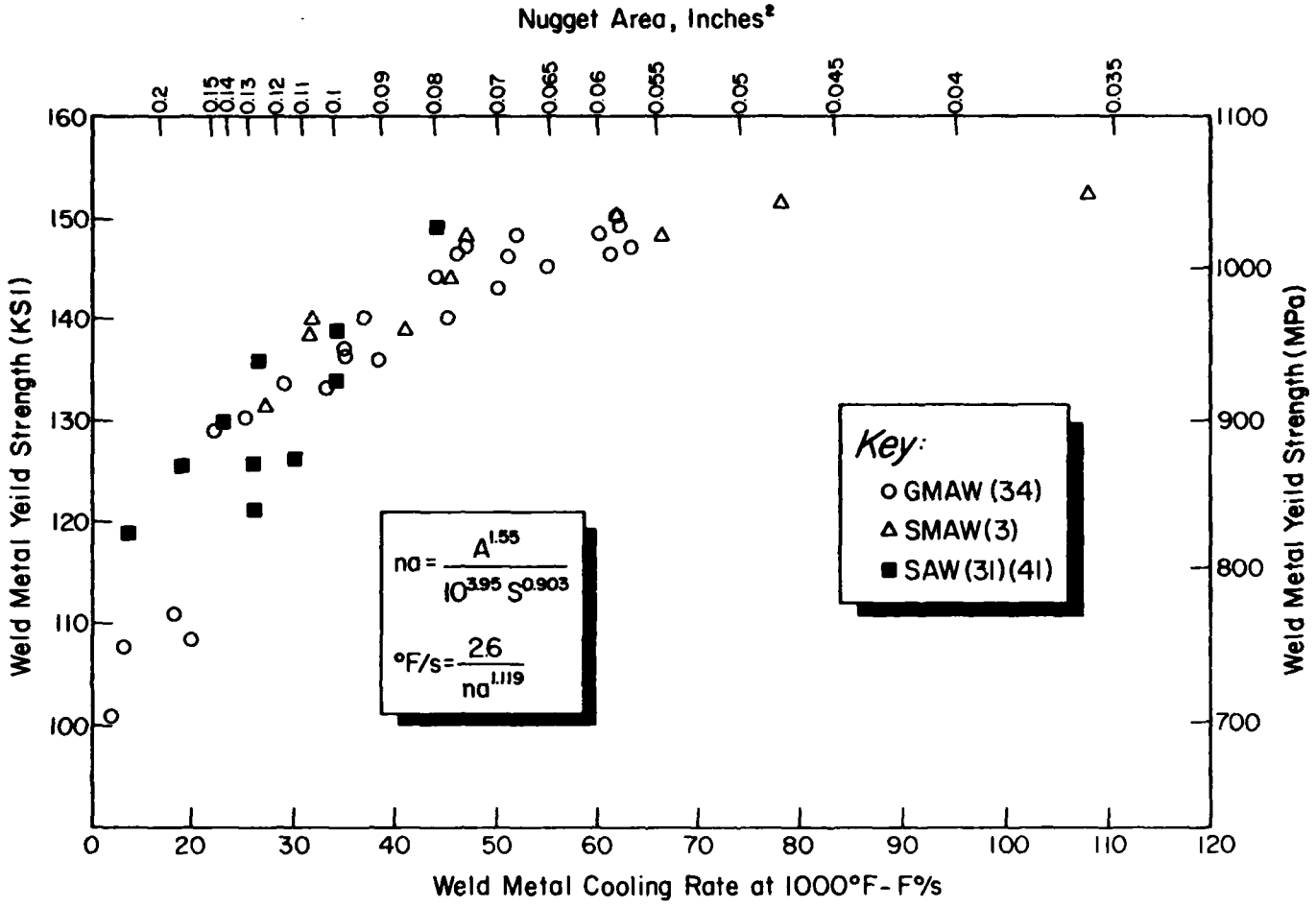

Figure 22. The Effect of Nugget Area and Weld Metal Cooling Rate on Weld Metal Yield Strength in HY-130 Steel Using Three Welding Processes.

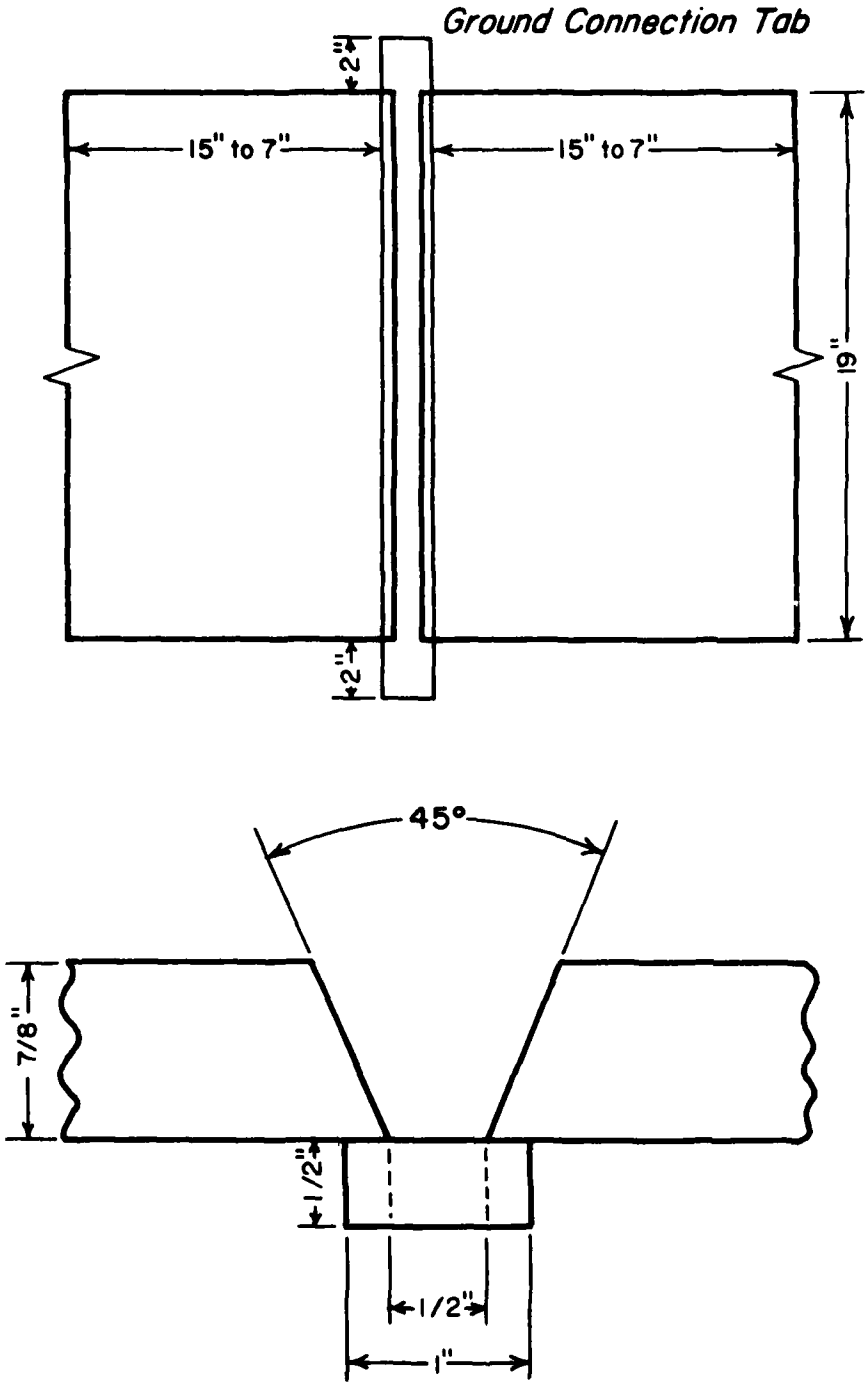

Figure 21. Joint Preparation Used for Mechanical Property Plates.

was performed by a commercial laboratory in accordance with ASTM Specification A 370. The results for two commercial fluxes and six experimental fluxes are given in Table 9.

The results of the mechanical property tests on these welds are shown in Table 9. Chemical analysis of the weld metals are shown in Table 10. Weld metal produced with commercial fluxes with the selected welding was low in yield strength. The experimental fluxes showed improved yield strength with low impact values. Initially this was attributed to high silicon content but, from results of MPS-10, even with silicon contents below 0.40% the weld metal failed to meet Navy specifications of 50 ft-lbs. at room temperature with 135 ksi minimum yield.

In order to determine the reason for the differences in properties, the weld joints were cross sectioned and polished. Photographs of weld cross sections appear in Figures 23 through 26. A difference in structure between the weld produced with a commercial flux (Figure 23) and welds produced with experimental fluxes is readily apparent. The weld produced with Flux B appears to have a finer structure with less columnar grains apparent in the last pass than for the experimental flux (Figure 24).

Photomicrographs were taken of the different structures of the welds. The coarseness of the weld metal microstructure of the experimental flux welds is apparent. Close examination of region A on several of the plates reveals a large amount of fine microcracks between the columnar grains.

The microstructures of the last pass in the welds produced with experimental fluxes appears to be made up of untempered martensite, lower

Plate Designation	Flux Used	Base/Acid Ratio	Yield Strength (ksi)	Tensile Strength (ksi)	Elongation in 2 in.(%)	Reduction In Area (%)	Hardness (Weld Metal) (R_c)	Room Temp Charpy-V ft-lbs
MPS-1	C(MgO-Al_2O_3-SiO_2)	3.85	126.07	138.90	18	58	24	58
MPS-3	VHP-II	1.78	134.44	149.50	15	44	34	37
MPS-5	B(MgO-Al_2O_3-SiO_2)	2.13	131.10	147.96	17	59	34	60
MPS-6	VHP-VI	3.59	135.88	155.26	21	59	38	40
MPS-8	EHP-VI	3.57	143.15	149.26	1.5	7	38	15
MPS-9	VHP-XIII	3.19	139.45	167.26	12.5	33	35	31
MPS-10	VHP-XXIV-BC	1.97	127.30	145.20	18	57	31	39
MPS-11	D(CaO-BaO-SiO_2)	1.53	126.07	145.90	17	57	30	54

Table 9. SAW Mechanical Property Test Results.

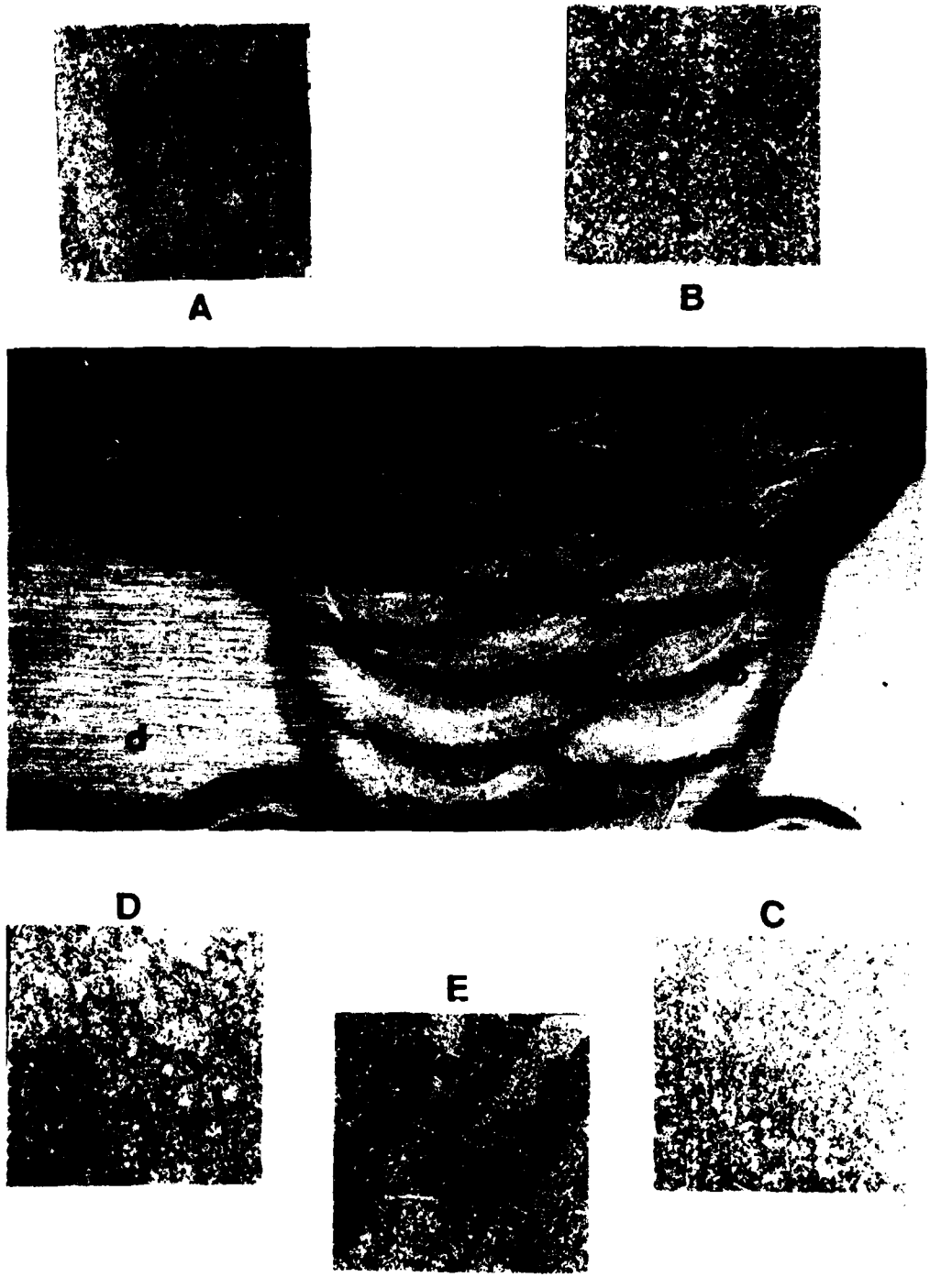

Figure 23. Micro and Macro Photographic Compositions MPS-5, Flux B.
Magnification: Macro 3X. Etchant: Ammonium Persulphate
Micro 100 X. Etchant: 2% Nital.

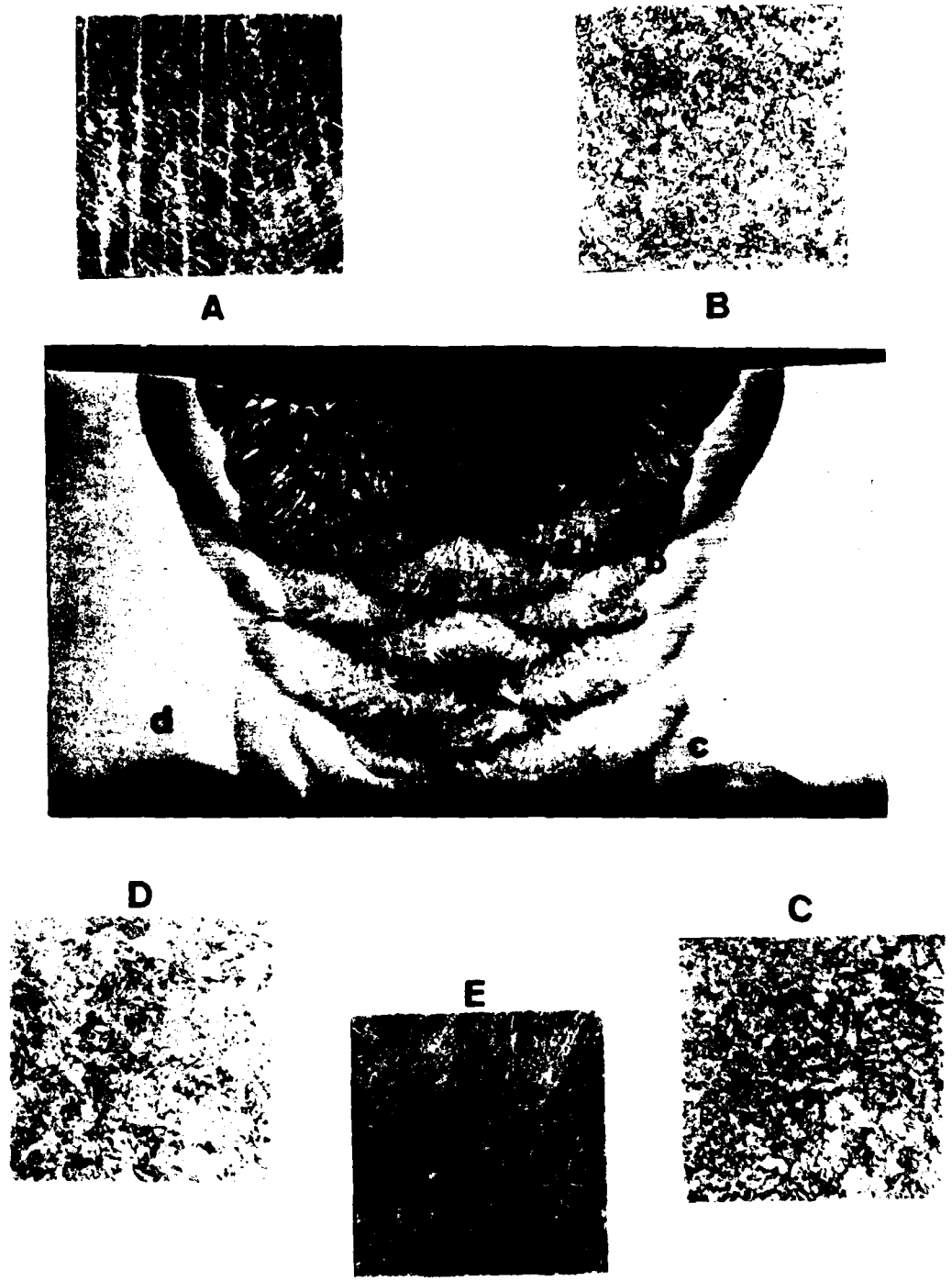

Figure 24. Micro and Macro Photographic Composite of MPS-6-Flux VHP-VI
Magnification: Macro 3X. Etchant: Ammonium Persulphate
Micro 100 X. Etchant: 2% Nital.

Figure 25. Macro Photograph of Cross Section of MPS-9-Flux VHP-XIII, Magnification: 3X. Etchant: Ammonium Persulphate.

Figure 26. Macro Photograph of Cross Section of MPS-8 flux EHP-VI, Magnification 3X. Etchant: Ammonium Persulphate.

bainite, ferrite and proeutectoid ferrite. Cracking originated in bands of ferrite (white) and propagated into the regions of untempered martensite and bainite. It is believed that the cracking observed is solidification cracking and may be related to the weld metal phosphorus content which exceeds the 0.010 limit for HY-130 in the case of the weld metal composition for the mechanical property plates (see Table 10).

The problem of cracking and low impact values associated with the very basic experimental fluxes was similarly encountered by Kirkwood (43) and Garland (19). These investigators attributed the problem to microstructures containing proeutectoid ferrite and upper bainite. Additions of vanadium and molybdenum were found to be effective for raising the toughness and transition temperatures. It is postulated that the solidification cracking may be due to a combination of effects. The welds produced with experimental fluxes have a pronounced columnar structure with large grains in the last pass bead. The low oxygen potential fluxes may produce weld metals with alloying elements richer than anticipated. The segregation of these alloying elements at solidification boundaries coupled with the existence of proeutectoid ferrite in these areas may be responsible for the cracking and lowered toughness.

The time and efforts required to investigate even a small item of interest are large when working with experimental fluxes. A single program only scratches the surface of the potential available with expanding flux-slag-metal technology. Increased research efforts are vital if these potentials are expected to be realized. The submerged arc welding process should produce weld metal of vacuum melted quality once the complex functions of a welding flux are understood.

Plate Designation	C	Mn	Si	S	P	N	O
MPS-1	0.10%	1.03%	0.19%	0.010%	0.015%	0.0092%	0.0232%
MPS-3	0.10	1.09	0.48	0.015	0.012	0.0070	0.0262
MPS-5	0.09	1.16	0.33	0.006	0.012	0.0106	0.0221
MPS-6	0.13	1.20	0.48	0.008	0.014	0.0056	0.0149
MPS-10	0.07	1.07	0.35	0.006	0.024	0.0077	0.0448
MPS-11	0.08	1.12	0.38	0.006	0.020	0.0073	0.0370

Table 10. SAW Weld Metal Chemical Analyses

Conclusions

The following conclusions can be substantiated from the material that has been studied.

1. Flux compositions based on the $MgO-Al_2O_3-SiO_2$ system were found to have adequate furnacing and welding performance at selected parameter levels. Composition ranging from 30 to 35% MgO, 16 to 24% Al_2O_3, 12 to 16% SiO_2 and 15 to 25% CaF_2 was found the most suitable. The addition of 5 to 10% barium carbonate was found to enhance the welding performance of these fluxes. Raw material purity was found to have a noticable effect on oxygen content. As the purity of the raw materials increased, the weld metal oxygen content decreased.

2. Increased flux basicity was found to decrease the weld metal oxygen content. Special flux additions such as ZrO_2 decrease the weld metal oxygen content. $BaCO_3$ when added as a mixture in amounts of 5 to 10% was found to be effective in lowering weld metal oxygen content.

3. Mechanical property weldments using 400 to 410 amperes, 28 to 31 volts and 14 to 15 inches per minute travel were made for two commercial fluxes. A yield strength of over 135 ksi was obtained with the experimental fluxes although the impact strength was low. The impact strengths for the commercial fluxes met a specification of 50 ft-lbs. at room temperature although the yield strength was low. The results of yield strength for these tests confirm the metallurgical influence of nugget area (which controls the cooling rate) on the values obtained. Further investigation of the effect of composition of an electrode for submerged arc welding of high strength steels is suggested.

4. Microstructural studies in this program indicate the low impact values with experimental fluxes may be attributed to the existence of solidification cracking in excessive amounts of proeutectoid ferrite in the matrix. The low oxygen potential fluxes may produce weld metal with alloying elements richer than anticipated. Segregation of these alloying elements at solidification boundaries coupled with the existnece of proeutectic and ferritic structures in these areas may be responsible for cracking and low toughness.

5. Results indicate that CaF_2 may be considered as a neutral component in the base/acid ratio calculations. A study of the effect of welding voltage which determines the amount of flux used does not affect the weld metal oxygen

or silicon content. Finally, the addition of ferroalloy powder to the weld zone did not decrease the oxygen content of the weld metal. The oxygen content appeared to be controlled almost entirely by the flux composition used in these tests.

James T. Hickey

Michael D. Hayes

Clarence E. Jackson

Bibliography

1. Jackson, C. E., Fluxes and Slags in Welding. WRC Bulletin 190, Welding Research Council, December 1973.

2. Jackson, C. E., The Science of Arc Welding. Welding Journal, 39, pp. 129-s to 140-s, 177-s to 190-s, 225-s to 230-s (1960).

3. Shultz, B. L., and Jackson, C. E., Influence of Weld Bead Area on Weld Metal Mechanical Properties. Welding Journal, 52, (1) pp. 26-s to 37-s (1973).

4. Adams, C. M. Jr., Heat Flow in Welding. Welding Handbook Volume 1, Sixth Edition, pp. 80-98, 1976.

5. Claussen, G. E., The Metallurgy of Covered Electrode Weld Metal. Welding Journal 28(1), pp. 12 to 24 (1949).

6. Christensen, N. and Chipman, J., Slag-Metal Interaction in Arc Welding. WRC Bulletin 15, Welding Research Council, 1953.

7. Erokhin, A. A., Temperature of Molten Electrode Metal Drops During Arc Welding. Izvest. Akad. Nauk SSSR, Otdel.Tekh. Nauk, No. 9, 125-136, September, 1955.

8. Pokhodnya, I. K. and Frumin, I. I., The Temperature in the Weld Pool, Automatic Welding, 14, May, 1955.

9. Awdo, Kohei and Nishiguchi, Kinuzuki. Average Temperature of the Molten Pool in TIG and MIG Arc Welding of Steel and Aluminum. IIW Document 212-161-61, 1968.

10. Davis, M. L. E., and Coe, F. R. The Chemistry of Submerged Arc Welding Fluxes. The Welding Institute, Research Report. May 1977.

11. Weast, R. C., Handbook of Chemistry and Physics. Section D, Thermodynamic Properties of the Oxides. The Chemical Rubber Co. 1976.

12. Elyutin, V. P., Pavlov, Yu. A., Levin, B. E., and Alekseer, E. M. Production of Ferroalloys-Electrometallurgy. Office of Technical Services U.S. Department of Commerce. Translation OTS-61-11429, 1957.

13. Jackson, C. E. and Shrubsall, A. E. Submerged Arc Welding of Chromium-Bearing Steels. Welding Journal, 33(8), pp. 752-758 (1954).

14. Zeke, Julius. A contribution to the way of Expressing the Welding Flux Basicity. IIW Document XIIE-61-80, 1980.

15. North, T. H., Bell, H.B., Nowicki, A. and Craig, I. Slag/Metal Interaction, Oxygen and Toughness in Submerged Arc Welding, Welding Journal 57, (3), 63-s to 75-s (1978).

16. Eagar, T. W. Sources of Weld Metal Oxygen Contamination During Submerged Arc Welding. Welding Journal, 57 (3) 76-s to 80-s (1978).

17. Boniszewski, T. Basic Fluxes and Deoxidation in Submerged-Arc Welding of Steel. Metal Construction, British Welding Journal, 6, (4), pp. 128-129 (1974).

18. Tuliani, S. S., Boniszewski, T. and Eaton, N. F. Notch Toughness of Commercial Submerged-Arc Weld Metal. Welding and Metal Fabrication 37, 327-339, 1969.

19. Garland, J. G., Kirkwood, P. R. A Reappraisal of the Relationship between Flux Basicity and Mechanical Properties in Submerged-Arc Welding. Welding and Metal Fabrication (4) pp. 217-224, 1976.

20. Bennet, A. P. Using Basic Fluxes, Metal Construction and British Welding Journal, 2(12), pp. 523-527, 1970.

21. Mills, K. C. and Keene B. J. Physicochemical Properties of Molten CaF_2-based Slags. International Metals Reviews (1) pp. 21-69, 1981.

22. Mori, Kazumi. A New Scale of Basicity in Oxide Slags. Bulletin of the Faculty of Engineering, Ibaraki University, Vol. 2, pp. 45-56, 1960.

23. Jones, L. Y., Kennedy, H. E. and Rotermund, M. A. Electric Welding, U. S. Patent #2,043,960, June 9, 1936.

24. Levin, E. M., Robbins, C. R., McMurdie, H. F. Phase Diagrams for Ceramist, American Ceramic Society 1964, Supplements published in 1969 and 1975.

25. Miller, W. B. Electric Welding Medium, U. S. Patent #2,228,639, January 14, 1941.

26. Hilty, C. C., Farley, R. W. and Girardi, D. J. Electric Furnace Steel-making, Volume II, Theory and Fundamentals. American Institute of Mining, Metallurgical, and Petroleum Engineers, 1963.

27. Duckworth, W. E. and Hoyle, G. Electroslag Refining. Chapman and Hall Ltd. 1969.

28. Bodsworth, C. and Bell, H. B. Physical Chemistry of Iron and Steel Manufacture. Longman Group Ltd. 1972.

29. Pehlke, R. D., Porteer, W. F., Urban, R. F., and Gaines, J. M. BOF Steelmaking Volume Two. Theory. American Institute of Mining, Metallurgical, and Petroleum Engineers. 1975.

30. Dorschu, K. E. and Lesnewich, A. Development of a Filler Metal for High Toughness Alloy Plate Steel with a Minimum Yield Strength of 140 ksi. Welding Journal, 43(12), pp. 564-s to 576-s (1964).

31. Kohns, R., and Jones, S. B. An Initial Study of Arc Energy and Thermal Cycles in the Submerged Arc Welding of Steel. Research Report. The Welding Institute, 1978.

32. Krause, Gregory T. Heat Flow and Cooling Rates in Submerged Arc Welding. Master's Thesis, Ohio State University, Department of Welding Engineering, 1978.

33. Niles, R. W. and Jackson, C. E. Weld Thermal Efficiency of the GTAW Process. Welding Journal, 55(1), pp. 25-s to 32-s (1975).

34. Connor, L. P., Rathbone, A. M. and Gross, J. H. Development of Procedures for Welding HY-130(T) Steel, Welding Journal, 46(7), pp. 309-s to 321-s (1967).

35. Rosenthal, D. Mathematical Theory of Heat Distribution During Welding and Cutting. Welding Journal, 20(5), pp. 220-s to 234-s, (1941).

36. Jackson, C. E. Control of Some Weld Metal Properties for Quenched and Tempered Steels, IIW, IXG-245-71, 1971.

37. Jackson, C. E. and Shrubsall, A. E. Progress Report on Development of $MgO-Al_2O_3-SiO_2$ Unionmelts for Heavy-Current Welding. October 24, 1948 and Report #2 on $MgO-Al_2O_3-SiO_2$ Melts for High-Current Welding. June 29, 1949. Union Carbide Research Laboratories Inc. Niagara Falls, New York,

38. Maykuth, C. L. The Deoxidation of Weld Metal Using Metal Powder Additions in Bulk-welding. Master's Thesis, Ohio State University, Department of Welding Engineering, 1979.

39. Koukabi, A. H., North, T. H., and Bell, H. B. Properties of Submerged Arc Deposits-effect of Zirconium, Vandium and Titanium/Boron. Metal Construction 11(12), pp. 639-644, 1978.

40. Belton, G. R., Moore, T. J. and Tankins, E. S. Slag-Metal Reactions in Submerged-Arc Welding, Welding Journal 42(7), pp. 289-s to 297-s (1963).

41. Wills, R. E. An Examination of the Mechanical Porpoerties of Submerged Arc Welds of HY-80 and HY-130(T) Steel. Master's Thesis, Ohio State University, Department of Welding Engineering, 1972.

42. Uwer, D. and Degenkolbe, Joachim. Characterisation of the Influence of Welding Temperature Cycles on the Mechanical Properties of Welded Joints TSISI translation 17086. Stahl and Eisen 97, (24), pp. 1201-1207 (1977).

43. Kirkwood, P. R. and Garland, J. G. The Influence of Vanadium on Submerged Arc Weld Toughness, Welding and Metal Fabrication, (2), pp. 17-28, 93-99, 1977.


DATE
ILME